

## Modelling of defects in aluminium cast products

Jolly, Mark; Katgerman, Laurens

**DOI**

[10.1016/j.pmatsci.2021.100824](https://doi.org/10.1016/j.pmatsci.2021.100824)

**Publication date**

2022

**Document Version**

Final published version

**Published in**

Progress in Materials Science

**Citation (APA)**

Jolly, M., & Katgerman, L. (2022). Modelling of defects in aluminium cast products. *Progress in Materials Science*, 123, Article 100824. <https://doi.org/10.1016/j.pmatsci.2021.100824>

**Important note**

To cite this publication, please use the final published version (if applicable). Please check the document version above.

**Copyright**

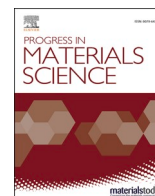
Other than for strictly personal use, it is not permitted to download, forward or distribute the text or part of it, without the consent of the author(s) and/or copyright holder(s), unless the work is under an open content license such as Creative Commons.

**Takedown policy**

Please contact us and provide details if you believe this document breaches copyrights. We will remove access to the work immediately and investigate your claim.

Contents lists available at [ScienceDirect](https://www.sciencedirect.com)

## Progress in Materials Science

journal homepage: [www.elsevier.com/locate/pmatsci](http://www.elsevier.com/locate/pmatsci)

## Modelling of defects in aluminium cast products

Mark Jolly<sup>a,\*</sup>, Laurens Katgerman<sup>b,a</sup><sup>a</sup> Cranfield University, Cranfield, UK<sup>b</sup> Delft University of Technology, Delft, the Netherlands

## ARTICLE INFO

## Keywords:

Computer numerical simulation  
Modelling  
Defects  
Cracks  
Segregation  
Porosity

## ABSTRACT

Over the last 4 decades, remarkable progress has been made in the modelling of casting processes. The development of casting models is well reflected in the proceedings of the 15 Modelling of Casting, Welding and Advanced Solidification Processes (MCWASP) conferences that have been held since 1980.

Computer simulations have enabled a better understanding of the physical phenomena involved during solidification. Modelling gives the opportunity to uncouple the physical processes. Furthermore, quantities that are difficult or impossible to measure experimentally can be calculated using computer simulations e.g. flow patterns and recalescence. However, when it comes to accurately predicting casting performance and in particular, the occurrence of defects like cracks, segregation and porosity there is certainly some way to go.

In this paper, the current understanding of the main mechanisms of defect formation during shape and DC casting processes will be reviewed and requirements will be discussed to give a direction to making casting models more predictive and quantitative.

## 1. Introduction

## 1.1. History

Casting is a prehistoric process, but it is thought to be predated by wrought metals, because the temperatures required to achieve the molten metal are far higher than those needed for wrought processes. Shape casting is a process by which metal is transformed from ingot or scrap to a shape that has added value and is close to the final shape of the object required by a designer. Shape castings can be used without any final finishing or can be fully machined, making both the surface and internal integrities important. Shape casting is essentially a batch process, even though modern engineering techniques have been applied to many processes to automate them. This is in direct contrast to continuous casting of steel or the so-called continuous casting of aluminium and its alloys developed in the 20th century. Continuous direct chill cast (DC cast) aluminium is actually a semi-continuous process. The largest ingots produced to date are “Jumbo” slabs 2700 mm by 610 mm [1] and round billets 1050 mm (42”) diameter × 7 m weighing 20 tonnes [2]. In both of the continuous processes, the final product is usually the feedstock for some other forming process, such as rolling, forging, machining or extrusion. Simulation and modelling of casting processes is a technique that has been developed over the last 5–6 decades in order to give casting engineers a tool to control the quality of the end products they are making.

\* Corresponding author.

E-mail address: [m.r.jolly@cranfield.ac.uk](mailto:m.r.jolly@cranfield.ac.uk) (M. Jolly).

<https://doi.org/10.1016/j.pmatsci.2021.100824>

Received 14 August 2020; Received in revised form 19 May 2021; Accepted 24 May 2021

Available online 28 May 2021

0079-6425/© 2021 The Authors. Published by Elsevier Ltd. This is an open access article under the CC BY license

(<http://creativecommons.org/licenses/by/4.0/>).

**Table 1**  
Summary of main aluminium alloys for shape casting and DC Casting.

Series	Main Alloying Elements	Typical Freezing range (°C)	Series	Main Alloying elements	Typical Freezing range (°C)
1xx.x	Al > 99%	<1	1xxx	Al > 99.5%	<1
2xx.x	Cu	<20	2xxx	Cu 2–6% total additions < 7%	15
3xx.x <sup>a</sup>	Si with Cu and/or Mg	1–50	3xxx	Mn < 1.5% total additions < 2.2%	140
4xx.x	Si	1–50	4xxx	Si < 6% (usually)	25
5xx.x	Mg	40–60	5xxx	Mg < 5% (Mn < 1%) total additions < 6%	65
6xx.x	Unused	–	6xxx	Si < 1.4% Mg < 1.1% total additions < 4.3%	50
7xx.x	Zn	10	7xxx	Zn < 11% Mg < 3.3% (Cu < 2.3%) total additions < 15%	155
8xx.x	Sn	370	8xxx	Fe < 8.6% (Li < 3%) total additions < 12.5%	
9xx.x	Other alloys elements	–	9xxx	Unused	

<sup>a</sup> Alloy additions can be as high as 30 wt% for example A39x (high silicon alloys) in which case the freezing range is over 220 °C.

## 1.2. Casting processes

### 1.2.1. Shape casting

Shape casting entails the manufacture of a mould or die as a three-dimensional (3D) “negative” form of the shape that is required to be cast. In other words, where a hole is required a “core” is used to make that hole; where a boss is needed a cavity is made in the mould. Having manufactured the mould from suitable material, for example sand, ceramic, or steel, liquid metal is channelled into the mould cavity through the “running system” and allowed to solidify. The running system is an integral part of the casting when made but is usually cut off or “fettled” when the casting is cold enough to handle. Other features are added to the casting in an attempt to produce sound products. “Feeders” are placed on the casting to act as reservoirs of molten metal, to counteract the natural solidification shrinkage that most metals experience on freezing. These feeders are then removed during the fettling. The design of the extra parts that are added to the shape of the finished component, i.e., the feeders and running system, are known in the USA as the “rigging” and in the UK as the “method.” The whole process of shape casting is often also known as “founding” and the manufacturing plants as foundries. Beeley [3] has written a useful text book on Foundry Technology for those wishing to understand more about the processes of founding.

From the standpoint of a physicist, the shape-casting process is transient until the casting reaches room temperature. This is unlike the continuous casting processes, which do have long periods of time during which the process is almost at equilibrium.

For the engineer, a transient process contains inherent problems, mainly of control. In order to help reduce manufacturing problems within the foundry sector, many alloys have been developed specifically for shape casting. These alloys have elements added to enhance fluidity (the ability to flow), e.g., silicon in aluminium alloys. This is again a difference compared with continuous casting processes, where usually the wrought alloy composition is cast. Table 1 is a comparison of the nominal compositions of shape-cast and wrought alloys with the approximate freezing ranges which drives the solidification and influences the modelling of these alloys from a

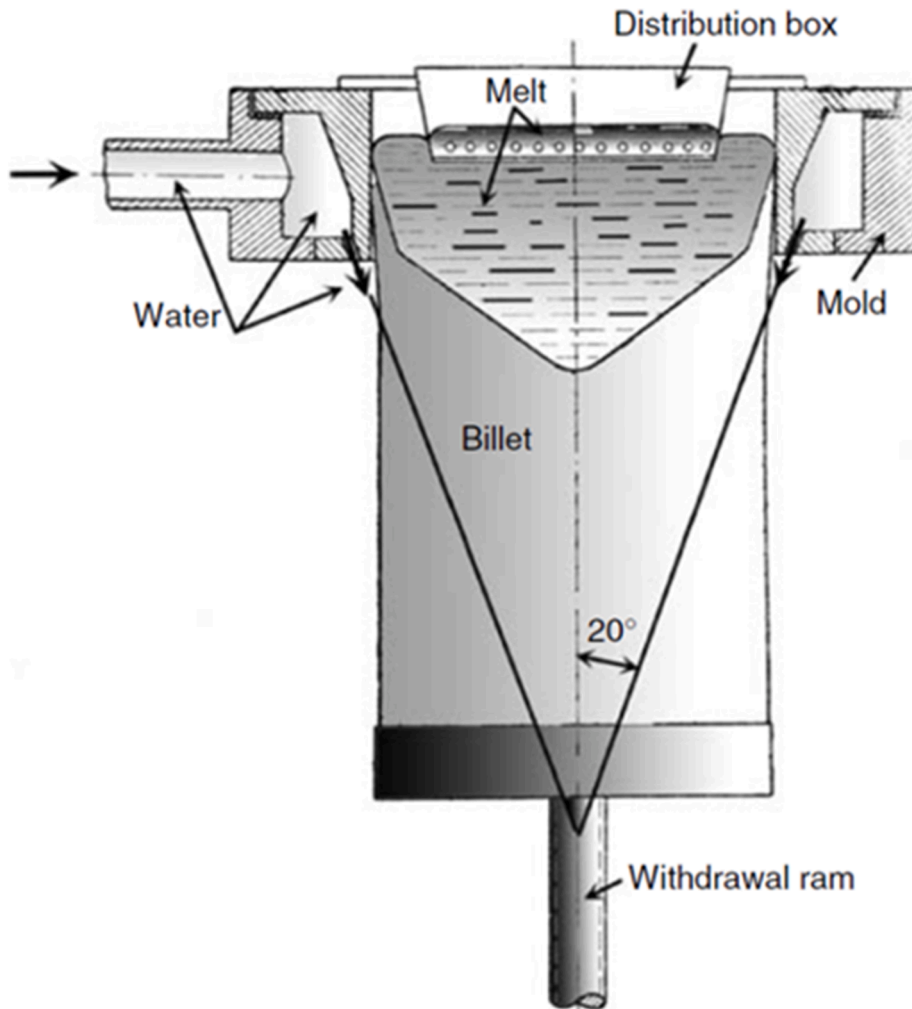


Fig. 1. DC casting set-up [7].

metallurgical respect.

### 1.2.2. Direct-Chill (DC) casting

DC casting of aluminium alloys, which was developed around 1930, was put into application due to the needs of the aircraft industry for the mass production of large billets (both round and rectangular). Prior to that the aluminium industry used permanent moulds or book moulds for making ingots similar to the steel industry. DC casting was invented independently by VAW (Germany) [4] and Alcoa (USA) [5] and is nowadays used to cast sheet ingot (up to  $500 \times 1500\text{--}2000$  mm) and round ingot (up to 1100 mm in diameter) for subsequent rolling, extrusion or forging respectively. Continuous sheet casting processes can produce sheet directly with a minimum thickness of about 3 mm and eliminate the costly hot rolling operation. Because continuous casting is limited to alloys with a narrow freezing range, DC casting process remains the main ingot casting method to produce aluminium alloys. Details of DC casting technology are extensively discussed in Refs [6] and [7]. Fig. 1 is a schematic of the process.

In the direct-chill casting process liquid metal is being fed into a water-cooled mould (primary cooling) where a solidified shell is formed with sufficient mechanical strength to contain the molten core at the centre. At the start of a casting a stool-cap or starter block is placed into the mould. By lowering the stool-cap, the ingot emerges from the mould and water impinges directly on the cast surface (secondary cooling) and completes the solidification process. The solidifying ingot descends steadily into the pit until it reaches full length. The metal level in the mould is controlled with a float system. During solidification, the shrinkage pulls the metal away from the mould to form an air gap and significantly reduces the heat extraction from the mould. Depending on the casting speed and length of mould, partial remelting of the solidified shell can occur before secondary cooling takes place. Secondary cooling accounts for about 95% of the overall cooling of the ingots. In a modern DC casting installation up to hundred extrusion billets or ten rolling ingots can be cast simultaneously.

### 1.3. Casting defects

Defects arising during the casting of aluminium alloys dramatically affect the mechanical and physical properties of the final cast product. Defects form due to a range of mechanisms, such as surface oxidation, entrainment, incorporation of exogenous materials from the containment vessels, dissolved gasses, solidification shrinkage, unwanted micro-structural phases with detrimental morphologies, and the development of stresses in the solidifying metal. The mechanism for the generation of most defects arises from a combination of many physical processes. Understanding of the mechanisms that generate the defects is fundamental in being able to control them and therefore produce better quality end products. Fig. 2 illustrates some examples of defects in cast aluminium alloys and the approximate length scales at which they occur.

Currently, a wide variety of aluminium alloys is being cast on a routine base by means of several casting processes and length and time scales as detailed in Table 2. However, in search for better properties such as a higher corrosion resistance or a higher strength, new compositions are being developed which may impose strict constraints on the process window. Not only should the process parameters such as casting temperature, cooling rate and mould filling should be controlled accurately, but a profound knowledge of the behaviour of the alloy during the casting process is required in order to produce a defect-free ingot or casting.

In general, defects occurring during casting can be divided into external and internal defects. The most common defects are shown in Table 3.

It is clear from Tables 2 and 3 that the differences in length and time scales in DC casting and shape casting. The more transient behaviour associated with shape casting processes leads to a wider range of defects. There are some common defects driven by the same processes and these are shown emboldened in Table 3. In DC casting defects occur mainly due to the strong thermal gradients in the ingot. During the production of wrought ingots removal of inclusions and oxides as well as degassing are widely applied and consequently the occurrence of oxides and porosities are well controlled. However, for the high-performance alloys cracking and macro-segregation can be a major problem. Macro-segregation originates from buoyancy driven flow in the sump where thermal stresses may lead to distortion of the ingot shape (e.g. butt curl, butt swell, rolling face pull-in) and possibly to hot tearing or cold cracking. In general macro-segregation does not occur in shape casting.

### 1.4. Modelling and simulation of casting processes

Casting of metals is a highly complex process due to the interaction of various phenomena. The challenge is to determine the optimal processing parameters to produce a casting, which meets demanding performance requirements. To achieve this objective process modelling has become an essential tool to understand the underlying physics and to produce consistent products.

During casting transport phenomena as heat flow, mass flow and fluid flow are highly coupled. Casting modelling is done at nearly all the size scales for the physical processes involved: nucleation, dendrite tip growth, liquid metal flow through a mushy semi-solid dendritic network, etc. [9]. Broadly speaking, casting modelling can be considered at two distinct length scales [10]:

- Macroscopic scale of the process over which the governing transport equations of heat, mass, momentum and deformation are valid
- Local scale at the solid–liquid interface where the solidification phenomena are operative

Modelling activities at macroscopic level describe the phenomena with a typical length scale in the order of the dimensions of the casting (1 mm – 1 m). Overall velocities, temperatures and stresses are calculated by numerical methods coupling temperature, fluid velocities and stresses in the solid [11,12]. The as-cast microstructure, which is very important for the properties of semi- and finished

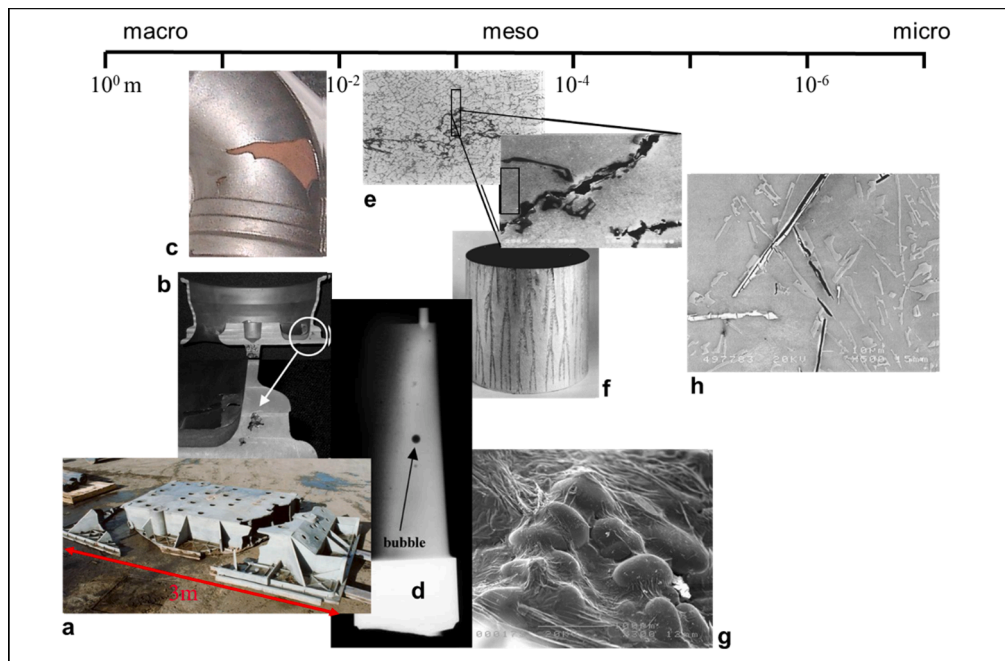


**Fig. 2.** Examples of defects in aluminium alloy castings. a) macro quench cracks in sand cast A356 as a result of residual stresses b) macro shrinkage in low pressure die cast LM25 c) non-fill in sand cast L99 d) atmospheric bubble in investment cast TiAl e & f) oxide films in die cast LM25 g) oxide film draped over primary dendrites in sand cast A380 h) micro-crack in the centre of Fe rich intermetallic needles in A356 [8].

**Table 2**  
Length and time scales of different casting processes used for aluminium alloys.

Process	Range of component Mass	Timescale of process
Direct Chill (continuous casting)	tonnes	hours
Sand	100 g to 5 t	Seconds to hrs
Investment (lost wax)	<10 g to 100 kg	Minutes to hours
Shell mould casting	100 g to 100 kg	Minutes to hours
Gravity Die (permanent mould)	1 kg to 50 kg	Minutes
Low pressure die	2 kg to 30 kg	Minutes
High pressure die casting (die casting)	10 g to 30 kg	Seconds to minutes
Squeeze casting	100 g to 20 kg	Minutes

**Table 3**  
Defects commonly found in cast aluminium alloys.

External Defects	DC casting	Shape casting	Provenance <sup>a</sup>
Macro-shrinkage, sink and draw		X	T
<b>Cold shuts</b>	X	X	T&F
Mould erosion defects & exogenous inclusions		X	T &F
<b>Gas blows blows/pin holes</b>	X	X	T&C
<b>Casting dimensions &amp; distortion</b>	X	X	T&M
<b>Hot tearing/hot cracks</b>	X	X	T&M
Internal Defects	DC casting	Shape casting	Provenance <sup>a</sup>
<b>Porosity</b>	X	X	T
<b>Hot tearing/hot cracks</b>	X	X	T&M
<b>Cold cracking</b>	X	X	T&M
Macrosegregation	X		T&C
Entrained bubbles and oxide films		X	F&C
<b>Unacceptable microstructure(Grain size, orientation etc.)</b>	X	X	T&C

<sup>a</sup> Provenance indicates the main mechanism for controlling the defect. T: thermal; F: filling; M: mechanical; C: composition/chemistry.

products, has a length scale varying from 1  $\mu\text{m}$  to 100  $\mu\text{m}$ . Microstructural transformations at these length scales are modelled with a variety of meshed and lumped parameter models [13]. An integral casting model has to couple macroscopic models of the governing transport phenomena with micro-models of the process physics. A numerical simulation of the whole process, with a spatial resolution at the scale of the microstructure, would require at least  $10^{12}$  nodal points in three dimensions. Even with the current hardware and software tools, it becomes unrealistic to model a complete casting at the length scale level of the microstructure. The optimal coupling between micro-models and macro-models is a main field of interest of casting modelling research [14]. A recent review by Rappaz [15] has looked at the last 40 years of modelling microstructures in casting and concluded that there are still many materials properties that are not known, such as interfacial properties and energies, high temperature behaviours of materials and ordering, which hinder our understanding. However atomistic or molecular dynamical modelling will help contribute to this lack of knowledge.

Over the last few decades significant progress has been made in the field of solidification and casting modelling and this development is well documented in the 15 Proceedings of the Modelling of Casting, Welding and Advanced Solidification Conferences (MCWASP) since 1980 [16–31]. With increasing computer and processor power many aspects of the multi physics, coupled phenomena are now modelled at the macroscopic scale including free surface flow, heat and fluid flow and thermal stress. However, the implementation of these calculated results into real casting process windows and performance predictions is one of the key remaining challenges to make casting modelling truly successful and become a truly useful tool for manufacturing companies. Currently a major part of current casting modelling applications is used for the prevention of casting defects, for example the occurrence of porosity, thermal cracks and macro-segregation.

The solidification, heat and fluid flow and stress build-up during casting have been modelled to investigate the influence of the casting parameters and thereby to formulate recommendations for improvements in casting practice [12,32–39].

### 1.5. Modelling requirements

The following are considered as essential parts of a casting model:

- a spatial model of the geometry
- a set of transport equations, taking into account the significant physical mechanisms
- accurate boundary conditions
- thermodynamic database and thermo-physical and mechanical properties
- validation and interpretation of the computed results

#### 1.5.1. Geometry & representation

The action of dividing up the 3D solid geometry of a casting that is to be simulated is termed “discretization,” or more commonly “meshing”. Meshing is one of the most important aspects of the numerical methods approach and it can heavily influence the results obtained during the analysis cycle.. Dividing up the 3D geometry into discrete bits gives rise to numerous problems. For example, representing curved surfaces with cubes inevitably gives rise to steps which hamper any calculations that involve radiation, as the radiating surfaces are all at right angles to one another. Dividing up the object of interest into tetrahedra or irregular, six-faced cells (hexahedra) gives a more realistic model for the surface, but involves much more complicated mathematics, especially when dealing with conservation of mass or volume. However, in general, despite the complex mathematics, stress and flow problems are dealt better with the less rigid mesh structures, such as those that are hexahedron based. The usual method for representing curved surfaces is by classing a cell which is more than half full of material as full, and a cell which is less than half full as empty (usually termed Marker And Cell method, MAC) [40].

However one FDM-based code, Flow-3D from Flow Science Inc., Los Alamos, uses advanced mathematical algorithms to represent the free surface of both fluids and curved solids in a rectangular prismatic mesh. This method, termed Volume Of Fluid, or VOF method [41], represents a partially full cell by interpolating a surface across the cell in a way that is dependent upon the amount of material in the adjacent cells. This gives an excellent representation of the free surface.

#### 1.5.2. Process physics

There are a large number of physical processes that need to be modelled to cover all aspects of casting processes. These include the following: heat transfer; including radiation, convection, and conduction; mass transfer (mainly fluid dynamics), phase transformations, including solidification and subsequent solid-state changes and stress/strain behaviour; microstructural development; and segregation of chemical species.

The main governing equations for conservation of mass (continuity), momentum (fluid flow), and energy (heat flow) are extensively given in text books modelling of materials processing and casting [42–44]. In addition during solidification the release of latent heat has to be included e.g. as an equivalent specific heat [42]:

$$C'_p = C_p + L \frac{df_s}{dT} \quad (1)$$

where  $C'_p$  is equivalent specific heat,  $L$  is latent heat and  $f_s$  is fraction solid.

The fraction solid is a function of temperature and for binary alloys is given by the Gulliver-Scheil equation, while for complex alloys by a function fitted to DSC measurements of latent heat evolution [32].

To describe the coupled phenomena adequately, good insight in the physics of macrosegregation, flow in mushy media, and

constitutive behaviour at high temperatures is required. This implies very close interaction between controlled experiments and process physics formulation.

Key phenomena to be considered in a casting model are:

- (turbulent) forced and buoyancy driven flow
- free surface flow
- heat conduction and convection in liquid and solid metal
- liquid–solid phase change (release of latent heat)
- rejection, diffusion and convection of solutal alloying elements
- thermo-mechanical behaviour in mushy zone and solidified metal

The implementation of these key phenomena in the modelling approaches of the different casting defects is discussed in [Section 3](#).

### 1.5.3. Thermo-physical and mechanical data

Commercial alloys are multi-component and the description of their solidification paths have to be based on phase diagrams of multi-component alloys. Modellers have benefited from the rapid development of software such as JMatPro®<sup>1</sup>[45], Thermo-Calc or CALPHAD [46] in order to predict a number of these parameters where there is access to digital phase diagram data. Among the physical–mechanical properties, the permeability and constitutive behaviour at high temperatures in as-cast conditions are most difficult to obtain.

Accurate thermo-physical data input, such as solidus and liquidus temperatures, latent and specific heats, conductivity, viscosity, and surface tension, are important for obtaining good results. Some software packages provide the user with a selection of property data for most common alloys and moulding materials. It is often the case that there can sometimes be quite considerable errors in using these data, especially where properties are dependent on some other parameter such as the temperature, time or fraction solid.

Exotic or proprietary alloys can often cause a problem for modellers, as there is no universal database of thermo-physical data for general access. Data for standard alloys are relatively easy to find. Data for alloys with slight deviations from standard, or exotic alloys with low annual production tonnage and potentially with more casting problems, do not exist in the public domain and are extremely expensive to produce. This is where the previously mentioned property prediction software packages come into their own.

Thermo-physical data for moulding material properties for shape casting, especially for sand moulds or investment shell moulds, are not well documented [47]. Problems arise from the very fact that sand properties will vary from foundry to foundry. Investment shell technology is often unique to a foundry and regarded as a proprietary “art.” It is difficult to envisage how this issue can be resolved completely in modelling. Some headway is being made in this latter area by use of some simple, rule-based techniques, in order for foundries to be able to estimate certain thermo-physical data [48]. Such tools could be applicable to other situations in the foundry for example, mould coatings. Work on the modelling of sand core blowing will also contribute to a better understanding of the effect of cores during the casting process [49–51].

For DC casting the data for the aluminium moulds is relatively easy to obtain but where there are ceramic rings or distribution bags used they present a problem when the whole casting system is being modelled. This will often lead to a simplified model being used which doesn’t attempt to simulate the whole casting process.

**1.5.3.1. Constitutive behaviour of as-cast alloys.** Where thermomechanical data for a number of aluminium alloys are readily available, this unfortunately is not the case for alloys in as-cast conditions. To calculate the stress development during casting the availability of these properties is crucial. The first model to calculate thermal stresses during DC casting in a round ingot at steady-state used an elasto-plastic model [52]. The model follows Hooke’s law in the elastic region and assumes that in the plastic regime the plastic stress also increases linearly with increasing strain. More accurately the material behaviour in as-cast condition in the complete temperature range during casting can be expressed by the extended Ludwik equation [53–56]:

$$\sigma = K \varepsilon^{n_L} \left( \frac{\dot{\varepsilon}}{\dot{\varepsilon}_0} \right)^m \quad (2)$$

with  $\sigma$  the stress,  $K$  a material constant (i.e. the stress at  $\varepsilon = 1$  and  $\dot{\varepsilon} = 1 \text{ s}^{-1}$ ),  $\varepsilon$  the strain,  $n_L$  the strain hardening coefficient,  $\dot{\varepsilon}$  the strain rate,  $\dot{\varepsilon}_0$  a constant taken equal to  $1 \text{ s}^{-1}$  and  $m$  the strain rate sensitivity.  $K$ ,  $n_L$  and  $m$  can be determined from experimental data from room temperature to solidus temperature at the strain rates applicable to DC casting. For the higher temperature regime of the casting process, where the material deforms mainly by creep, experimental data can be fitted to the standard creep law:

$$\dot{\varepsilon} = A \sigma^n \exp\left(\frac{-Q}{RT}\right) \quad (3)$$

with  $\dot{\varepsilon}$  the strain rate,  $A$  a material constant,  $\sigma$  the stress,  $n$  the stress exponent,  $Q$  the activation energy,  $R$  the universal gas constant and

<sup>1</sup> JMatPro® is a simulation software which calculates properties for alloys and is aimed at multi-component alloys used in industrial practice. JMatPro® incorporates physically based materials models that have been extensively validated.



$T$  the temperature (K). This equation fits the data from creep tests in the temperature range 400–600 °C and the strain rate range  $10^{-6}$ – $10^{-2}$  s $^{-1}$  very well. The advantage of Eq.3 over Eq.2 is that the parameters are temperature independent and the temperature occurs explicitly in the equation.

The extended Ludwik equation takes into account both the strain rate sensitivity and temperature dependence of the stresses. Therefore, both the work hardening and creep behaviour can be captured. However, the model fails to capture the recovery that occurs during DC casting below solidus temperature. Recently Soni and Alankar [57] addressed this problem by analysing previously published stress–strain data fitted to the extended Ludwik equation [58]. The Voce equation [59] and Kocks–Mecking (KM) model [60] were used to predict the hardening and recovery behaviour during DC casting conditions. The KM model was able to fit the uniaxial tests within 1.5% of the regenerated data [57].

For the thermomechanical behaviour in the mushy zone the effect of liquid has to be taken into account and a modification of Eq. (3) is required. Braccini et al. applied [61] the exponential creep law to describe the semi-solid constitutive behaviour by assuming that the dendritic network takes all of the loading:

$$\sigma = \sigma_o \exp(\alpha f_s) \exp\left(\frac{mQ}{RT}\right) (\dot{\epsilon})^m \quad (4)$$

where  $\sigma$  is the stress,  $\sigma_o$  and  $\alpha$  are the materials constants,  $f_s$  is the solid fraction,  $m$  and  $Q$  are the strain rate sensitivity coefficient and activation energy, respectively,  $R$  is the gas constant,  $T$  is the temperature,  $\dot{\epsilon}$  is the strain rate.

Suyitno et al. [62] calculated the stress distributions during the steady-state stage in a round billet using Eq.4. During solidification, the radial and circumferential tensile stresses exist at the centre of the billet, while only circumferential tensile stresses occur at the periphery. This explains why hot tears most likely occur in the centre of a billet. Similar simulation results were reported by M'hamdi et al. [63].

Drezet and Eggeler [64] extended the exponential creep law to make the load carrying area directly proportional to the solid fraction:

$$\dot{\epsilon} = A \left(\frac{\sigma}{f_s}\right)^n \exp\left(-\frac{Q}{RT}\right) \quad (5)$$

$A$  is a materials constant,  $f_s$  is the solid fraction,  $n$  is the stress exponent. Considering the phenomenon that the low melting phases are located at grain boundaries, van Haaften et al. [65] replaced  $f_s$  with  $(1 - f_{LGB})$  where  $f_{LGB}$  is the amount of grain boundary area covered by liquid phases. The improved equation is expressed:

$$\dot{\epsilon} = A \left(\frac{\sigma}{1 - f_{LGB}}\right)^n \exp\left(-\frac{Q}{RT}\right) \quad (6)$$

The material parameters  $A$ ,  $n$ , and  $Q$  can be determined by the tensile tests at the solidus temperature.  $f_{LGB}$  is the fraction of grain boundaries covered with liquid. Wray [66] derived the dependence of  $f_{LGB}$  on solid fraction by assuming perfect wettability of the solid by the liquid. Consequently the predictions match well with the semi-solid tensile experiments for AA3104 and AA5182 [54] and AA6056 [67].

Subroto et al. [68,69] established the constitutive data based on the extended Ludwik and creep equations over the temperature range up to the solidus temperature for AA7050. This study was recently extended to include semi-solid parameters and failure behaviour of as-cast AA7050 [70].

Takai et al. explicitly included the dependence of the materials constants  $A$ ,  $n$  and the Young's modulus with temperature and fraction solid by applying Hooke's law and the visco-plastic Norton-Hoff law [71].

Phillion et al. [72,73,74] proposed a semi-solid empirical constitutive equation for AA5182 using a three-phase microstructure model. This constitutive model takes into account the effects of solid fraction, grain size and porosity fraction on the semi-solid tensile deformation. The constitutive law has been applied to simulate the DC casting process for AA5182 and investigate the effect of various microstructure features (grain size and rigidity point) and process parameters (casting speed) [75]. Furthermore Phillion et al. [76] studied the combination of X-ray radiography with semi-solid tensile deformation in Al–Cu alloys to establish mechanisms deformation and failure. A three-stage mechanism for semi-solid failure was proposed:

- strain localization and flow of liquid
- semi-solid necking
- formation of micro-necks, and final fracture

Tensile mechanical properties at various temperatures of as-cast or semi-solid samples are usually measured using a Gleeble-1500, 3500 or 3800 series thermo-mechanical simulator coupled with a modified tensile machine. Tensile specimens are heated through the Joule effect at a rate of 10 °C/s, kept for 10 s at temperature and then deformed at strain rates of  $10^{-2}$ – $10^{-4}$  s $^{-1}$  typical of DC casting [54,65,77,78,56,79] or the specimens are reheated from room temperature [56]. Both techniques led to the following general results. In several aluminium alloys it is observed that both strength and ductility strongly decrease from just below the solidus temperature to above solidus temperature, while the fracture surface changes from rough, related to the ductile behaviour, to smooth, related to the presence of a liquid film. Further, cracks initiate at micro-pores or molten inclusions and continue along grain boundaries Alternatively dedicated tensile machines are used to obtain constitutive properties [71] or to simulate DC casting mechanical behaviour [80–82].

#### 1.5.4. Boundary conditions

One of the most difficult aspects of any simulation exercise is the accurate representation of the boundary conditions. For all casting processes, the most important boundary condition is the thermal boundary condition. When casting simulation was first used in industry, most of the codes concentrated on the thermal aspects of the problem, excluding filling and liquid metal flow. Boundary conditions were relatively simple and heat-transfer coefficients, although not really known for material combinations, could be estimated for different mould materials. Initial temperature fields were often assumed to be isothermal which is a long way from the reality after the filling of the mould or die.

Boundary conditions are quite different for shape casting and DC casting. During DC casting three different cooling zones exist, the primary cooling and airgap in the mould cavity followed by the secondary zone below the mould by direct impingement of the water jets. In shape casting heat flow is complicated due to the interaction of mould filling and cooling. In addition, during solidification, aluminium shrinks away from the mould wall creating a gap with quite different boundary conditions dependant upon the local atmosphere. Clearly, the heat flux is a function of the process conditions and the surface temperature of the solidified shell.

Many of the current codes address mould filling, as well as the thermal aspects, and some have the capability to model stress. This immediately raises more issues with regard to boundary conditions. If stress models are used, then the heat transfer coefficients change over the time of the simulation and as a function of temperature as distortion occurs and gaps are created between the solidified metal shell and the mould or die.

The interface heat transfer coefficient ( $h$ ) is probably one of the most “fudged” parts of casting modelling. As the mould material properties are not accurately known, it is not possible to make accurate measurements of interface heat-transfer coefficients, although some attempts have been made [83]. Often the mould and the interface are treated as one and the same, even though there are certain mechanisms occurring which must change the value of  $h$  during the casting process. As previously discussed, the addition of die coats and mould washes will change  $h$ , and these should be taken into account in a more systematic way than is currently the practice. Often interface heat-transfer coefficients are used, which enable the user of the software to arrive at the correct defect prediction. Research has been carried out in order to be able to predict values of  $h$  [84]. A number of techniques have been used including inverse analysis [85,86] and so-called thermal resistor model which considers the air gap formation [87].

The initial boundary conditions for filling can be extremely complex and some of the issues are set out in the following. During an investigation at a UK crankshaft foundry, it was observed that during pouring of one single mould the inlet velocity could vary from  $1.7 \text{ m.s}^{-1}$  to  $2.2 \text{ m.s}^{-1}$  [88,89]. This is not untypical in a foundry and not dependent on the density of the alloy poured but the processes used which are similar across the shape casting sector.

When simulating any of the die-casting processes, it is usually necessary to impose an initial uniform temperature on the dies and then apply several (up to 10) solidification cycles in order to produce a temperature profile for the steady-state condition within the die, before completing a full analysis of filling and solidification.

Modelling of coatings (or paints) which may be no  $> 0.1 \text{ mm}$  thick is not really possible as the impact on the mesh size across the paint layer would make the overall mesh size massive. In order to influence the amount of heat transfer across the coating, a heat-transfer coefficient has to be obtained for the coatings used, and then applied to the surfaces which are coated. A review of coatings used in shape casting by Nwaogu and Tiejde [90] shows that *ab-initio* modelling of these materials would have little benefit. Representing the coating as a change in heat transfer coefficient from experimental data is the most sensible way [91]. The authors are not aware of a database of interface heat-transfer coefficients for materials combinations across the metal casting sector to represent coatings.

A number of authors have attempted to model heat flow in investment casting [92,93]. The major issues start from geometrical considerations. Often the aspect ratio of thinnest section to overall size of the casting is large. This therefore gives problems during the meshing stage. Other issues relate to the proprietary nature of the shell materials. Each foundry uses its own combinations of materials and therefore there is no databank of shell material. Radiation is a major consideration in this process, and so the software package must consider this aspect of heat flow, as well as conduction.

In lost foam casting, where pattern parts are glued together, there are problems in modelling from the glue material, which usually has very different properties from the bulk pattern properties. Other issues arise for the modeller in trying to model the decomposition of the polystyrene. However, researchers have attempted to address this problem [94,95]. Other results indicate that in thick sections the variation of density in the polystyrene can significantly change the way in which the liquid metal flows, and also influence the local thermal conditions [96].

When modelling high-pressure die-casting, the engineer has to be aware that, unlike in the other casting processes, because of the high velocities involved, often over  $80 \text{ ms}^{-1}$ , the metal stream does not stay coherent and is more likely to be like a spray of particles [97]. This has been replicated using smooth particle hydrodynamics (SPH) [98] which gave a better simulation of air entrainment than more conventional FD/FV based simulations. The air in the die is hugely influential on the filling pattern. Venting of the die is therefore essential and should be modelled. Although sand cores are not used in this process, some of the dies used are extremely complex and the section thicknesses can be very small (as low as  $0.1 \text{ mm}$ ). Sometimes additional post-filling pressure (intensification pressure) is applied by means of “squeeze pins” to specific locations in the casting. This is not easy to model although some black box software packages claim to have solutions [99]. Englada et al. [100] looked at the benefits of mould preheating cycles, whether it was necessary to model fluid flow as well as thermal flows and simplified geometry representation. They concluded that simplifying the geometry gave the most dramatic reduction in computation time by a factor of 10 with little loss in accuracy. However, it was important to ensure that the thermal profiles at the beginning of simulations accurately reflected reality.

### 1.6. Verification & validation

Verification is concerned with determining whether the conceptual simulation model is an adequate representation of the process. Modelling tools are mostly commercial products and coding and numerical robustness of the program are well tested. Models are validated by comparing the computed results with experimental data. This is relatively easily done for temperature profiles but is rather more complicated for liquid metal velocities and thermal stresses. Even more complex are defects such as porosity because of the range of scales ( $\mu\text{m}$  to  $\text{mm}$ ) and physical mechanisms this could cover [101–103], thermal contraction or dissolved gas such as

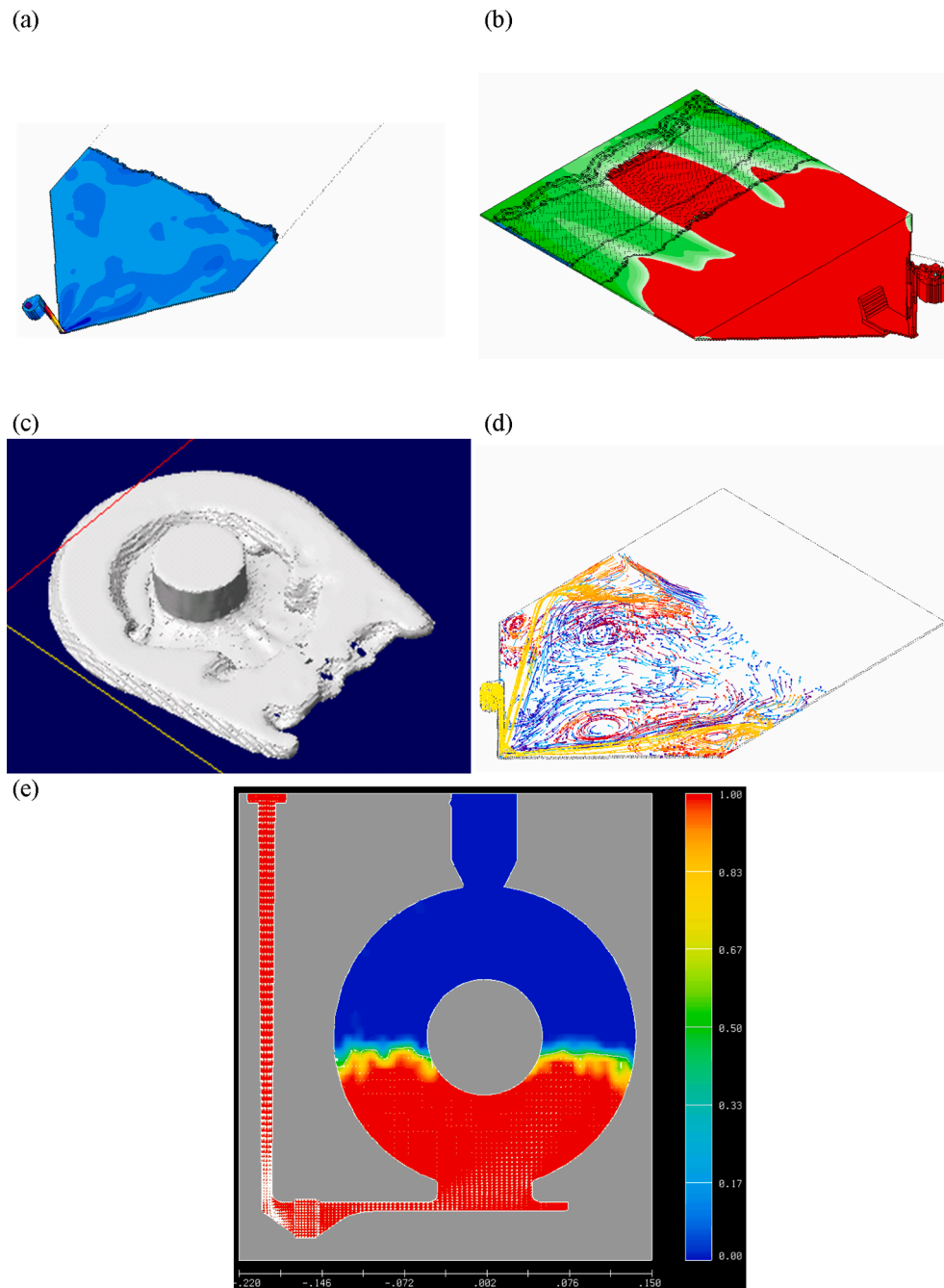


**Fig. 3.** (a) Velocity contours (light blue is low velocity, yellow is high); (b) liquid (red), mushy (green) and solid (blue) regions during filling of a plate; (c) rendered surface of liquid metal; (d) particle tracking enabling the interpretation of where inclusions might be washed to during the casting process, as well as indications of bulk filling history and the development of dead zones and eddies; and (e) a 2D cross-section through the liquid metal showing fraction of material and velocity vectors (white arrows) [117].

hydrogen [104,105]. Liquid metal entrainment defects (inclusions and gas bubbles) [106,11] and erosion of moulds become highly difficult although some attempts have been reported [107,108].

### 1.7. Prediction & sensitivity

The accuracy of the predictions made by simulation tools is highly dependent on the ability to capture the accurate boundary condition of the process and transient conditions that affect the physics during the phase change from liquid to solid. Casting processes are essentially 4D processes as time becomes extremely important during the filling, solidification and subsequent cooling. In a sensitivity analysis performed to examine the mould-metal heat transfer coefficient, mould thermal conductivity, wall friction factor, pouring basin pour temperature, and pouring basin head pressure through doing coupled flow simulations on thin-walled, castings using the commercial casting simulation software, MAGMASOFT concluded that results were highly sensitive to the thermo-physical data input [109]. In a sensitivity analysis on modelling of investment casting of LM25 Gebelin and Jolly [110] concluded that simulation results are highly dependent on the values of mould material heat capacity and heat transfer coefficients used. A further conclusion was that materials used in industry may behave differently to the behaviour in laboratory conditions where the data are often generated. Bolduc and Kiss [111] completed a sensitivity study to compare the effect of parameters that characterise boiling on hot tearing. The effect of input uncertainty in the modelling of high-pressure die casting has been investigated by Fu et al. [112]. Modelling results are most sensitive to the uncertainty in the interfacial heat transfer and the feeding effectivity. More recently Zindani et al. [113] presented a decision-making approach to handle the uncertainty concurrently with the fluctuations in data.

### 1.8. Interpretation of the simulation results

Computer simulation software is of no use unless the mass of information that is generated can be easily interpreted, so that the casting process can be changed in a controlled way to produce better cast products. However, much of what is seen in computer simulation is qualitative. There has been some research to develop quantitative methods of analysis using modelling as a tool to develop casting quality indices [114].

To couple calculated results to process performance requires both criterion functions for quantitative predictions and sophisticated visualisation techniques of 3D results. 3D vector quantities like velocities and stresses are difficult to represent and therefore post processing of the results can become very cumbersome. A challenge in modelling hence is to establish a quantitative link between modelling results and casting performance. Recent publications have focussed a number of parameters (including cost, quality, time and environmental sustainability) by using optimisation techniques [115].

Relating filling modelling to casting defects is probably the least-well-developed aspect of casting simulation. Results can be represented as velocity vectors, velocity contour maps (Fig. 3a), and temperature distributions (isothermals) in both 2D and 3D imagery (Fig. 3b). 2D images are cross-sections through the liquid and are often easier to understand than a fully transparent 3D model, even though a large number of sequential images are required to convey all the information about a filling system. Images of the free surface behaviour can also be useful (Fig. 3c). Surface turbulence using these images has to be interpreted. It is also possible to highlight all areas of the liquid metal that are above the critical velocity during any time-step. Particle tracing methods are also used to give some indication of the progression of fluid and the development of phenomena such as eddies or strong flow fields (Fig. 3d). Sometimes it is useful to present two sets of data, for example, fraction solid and velocity vectors (Fig. 3e).

A more recent development is the association of a scalar value with the free surface that has time dependence, and is associated with the oxide-generation mechanisms of free surface turbulence. This enables running systems to be evaluated more quantitatively. Fig. 3 illustrates some of the methods for showing filling in casting processes. Other research has investigated optimising melt velocity and effectively contribute towards the reduction of entrained air and surface defect concentration in the final cast product [116].

## 2. Modelling tools

A wide array of mathematical tools is applied to the physical models in order to solve the equations. These come in various guises and combinations of solutions, and include finite difference method (FDM) and finite volume method (FVM); finite element methods (FEMs); cellular automaton (CA) methods and lately, phase field theory [118].

The methods that can be employed for modelling a casting process broadly fall into four categories:

- heuristic or rule based
- analytical methods
- numerical methods
- stochastic methods

### 2.1. Heuristic

These software packages produce results without exposing the applied methodology for commercial reasons. There have been a number of these programs, like SOLSTAR, SoftCAST, and CADCAST. Some of them use a combination of home-grown rules and well-known criterion functions, such as the Chvorinov's [119] rule and modulus calculations. Others are more complex and less driven by

geometry. For example, in the late 1980s SOLSTAR predicted primary shrinkage and porosity in castings by first simulating heat flow through a finite-difference-type mesh in a full, 3D domain, and then by applying experimental criteria to the results. The materials' property data required by SOLSTAR were also empirical. This implied that SOLSTAR had to be calibrated for each alloy/mould combination and foundry practice.

## 2.2. Analytical models

A number of analytical solutions have been proposed in the past in order to help the cast metals engineer design the casting method. Those most well-known have been proposed by Chvorinov [119], who defined the concept of "modulus" (the ratio of volume to cooling surface area); by Wlodawer [120] (directional solidification); and by Niyama et al. [121] (prediction of centreline micro-shrinkage). Although these were largely developed for ferrous alloys they have also been used when dealing with Al alloys.

For DC casting algebraic relations are derived for sump depths as a function of casting speed or for the extent of macrosegregation depending on the alloy partition coefficient. In shape casting, prediction of hot spots, order of solidification and thus potential regions for porosity was historically assessed by calculating the so-called casting modulus of a different regions of the casting geometry. The casting modulus,  $M$ , was defined as the volume of the specified,  $V_c$ , region divided by the cooling surface area ( $A_c$ ) of that region and took no consideration of the alloy or mould materials [119]. This was later developed by Flemings to consider temperatures, conductivities and enthalpies of both mould and alloy cast to predict the solidification time for geometries with different shape factors [122].

$$S = \left\{ \frac{T_m - T_0}{H\rho_s} \right\} \left\{ \frac{2}{\sqrt{\pi}} \sqrt{K_m \rho_m C_m} + \frac{nK_m t_f}{2r} \right\} \quad (7)$$

$T_m$  is the melting point of the metal,  $T_0$  is the initial temperature of an infinite mould,  $\rho_s$  is the solid density of the metal,  $H$  is the latent heat,  $K_m$ ,  $\rho_m$  and  $C_m$  are the thermal conductivity, density and the specific heat of the mould,  $n$  is the shape factor constant, 0 for a plate, 1 for a cylinder, and 2 for a sphere.  $S$  gives us the thickness of solidified metal after any time  $t_f$ .

## 2.3. Numerical methods

Numerical methods like finite difference or volume (FVM) and/or finite element (FEM) are the most widely used due to the availability of workstations and sophisticated numerical software. The governing equations for casting processes are the conservation equations of heat, mass and momentum. These equations are well summarized in the literature, see for example [42]. The solidification process involves two phases: liquid transforms into solid, and solid moves through liquid and vice-versa.

### 2.3.1. Finite difference (FD)/finite volume (FV)/finite element (FE) methods

These names are given to a mathematical technique whereby the answer to a complex problem is obtained by dividing up the complete region (known as a domain) of the problem into small pieces (control volumes or elements), and then applying the equations to each of these pieces in turn. In FDM for each small volume, the calculation assumes that the material properties are the same over the complete volume. Consequently, for high accuracy the domain of calculation must be split into the highest number of cells possible, or practicable. Commercial software packages usually apply smoothing algorithms to the results obtained, to remove the steps that occur as a result of the small differences between adjacent control volumes. Thus the results are adjusted in a post-processing step to give smooth contours. The FDM calculations are carried out at predetermined time steps on an iterative basis. Results can be stored at the end of each time-step or after predetermined numbers of time-steps [42].

For FEM the materials properties used in the mathematical calculations are stored at the corners (nodes) of each element and sometimes at other places along the edges of the elements, for greater accuracy. The solutions are then obtained using these values to give a quantity (e.g., temperature) for these specific points (Gauss points) within the element. The positions of these points within the element are determined by the type of integration applied, the initial coordinates of the nodes, and the shape of the element. Unlike the FDM, the values of the variables used in the calculations are not considered as constant across the element, but are calculated by using some interpolation method. Time is taken into account iteratively and stepwise, in a similar fashion to the FDM. FEM has been well described in the literature [123].

It has been demonstrated that both FDM and FEM based programs can produce simulations of the modelling, the filling and solidification processes, to the same order of accuracy. It seems that both numerical methods are equally preferred by researchers studying filling and solidification modelling, as both FEM and FDM are capable of dealing with unstructured meshes. However, a survey by Jolly et al. [124] showed that over 50% of the programs used were FEM based, which certainly indicates to some extent that FEM is more popular, especially in the development phase. One major factor that has hindered the commercialisation of FEM packages has been mesh generation. In FDM packages this has always been relatively simple, but automatic meshing for FEM codes was not commercially available until 1995. Contrary to these findings are the facts that the most widely sold software packages used in the foundry industry on a worldwide basis are FDM based. FEM has advantages over FDM when thin-walled castings are of concern such as in investment casting or high pressure die-casting.

To obtain computed results from a casting model, dedicated or general purpose software can be used (for example MagmaSoft [125], ProCast [126], NovaFlow [127], AnyCasting [128], Solid/Flow/OptiCast [129] or Flow-3D [130] for shaped castings; ANSYS-CFX [131], ANSYS-FLUENT [132], Flow-3D [130] for fluid and heat flow phenomena; ANSYS [133], MARC [134] or ABAQUS [135]

for thermal stress problems).

The thermal and fluid flow fields are calculated by FVM or FEM using commercial CFD software packages like CFX, Flow3D, Fluent or dedicated programs like ALSIM<sup>2</sup> [136,137]. The effect of natural convection in the liquid metal is included through the Boussinesq approximation and turbulent effects are included using the  $\kappa$ - $\epsilon$  model or similar approaches. The transient heat and fluid flow effects during the start-up of DC casting have been modelled [138,139]. Thermo-mechanical aspects are usually modelled with commercial FEM packages like MARC [134], ANSYS [133], or ABAQUS<sup>3</sup> [135] although some of the dedicated shaped casting software also include these phenomena.

Sometimes there are also combinations of two techniques, such as the cellular automaton and finite element (CAFE) method proposed by Rappaz and his co-workers [140] (see also Section 2.4.1).

### 2.3.2. Meshless methods

The meshless or sometimes also named mesh free methods represent a class of numerical methods where an arbitrarily distributed set of nodes, without any additional topological relations between them, is used as an alternative to finite element or finite volume methods. The meshless method only requires a set of uniformly or non-uniformly distributed computational nodes inside the computational domain. Such meshless methods represent a promising technique to avoid problems with polygonisation. Several meshless methods are available, which are described elsewhere [141–143]. Smooth particle hydrodynamics is an example of one such meshless method has been used successfully by researchers for modelling process across the casting spectrum from the primary casting of foundry ingots to high pressure die casting where it successfully represented the breakup of metal streams into droplets and the subsequent potential oxide entrainment which is extremely difficult for meshed methods to achieve in order to resolve the droplet sizes [144].

## 2.4. Deterministic and stochastic models

In recent years studies on meso- and micro-modelling techniques in solidification science have increased rapidly. These studies largely concentrated to improve the understanding on [145]:

- anisotropic properties of the solid–liquid interface, including the solid–liquid interface free energy
- dendritic solidification with emphasis on orientation selection
- effects of convection on microstructure formation
- solidification at a high volume fraction of solid and formation of (micro) pores and hot tears

Microscopic models of solidification have been developed to describe the mechanisms of nucleation and growth of the solidifying phase. Beckermann and co-workers [146,147] coupled heat and mass flow equations with a microscopic model for equiaxed solidification. The temperature history as calculated in a macroscopic model is used as input for the microscopic model. Microstructural features, as dendrite arm spacing, are then deduced from local solidification time or other scaling laws. Micro-macro models are used to describe macrosegregation in DC ingots but have difficulty to model morphology changes such as the columnar-equiaxed transition. Furthermore, micro–macro models are based upon a deterministic approach: the number of grains and the growth of grains is a unique function of the thermal history and metal properties. The development of solidification microstructural models is discussed in two recent reviews by Kurz, Fisher and Trivedi [148] and Kurz, Rappaz and Trivedi [149].

### 2.4.1. Cellular automaton models

Deterministic solidification models can only predict certain aspects of microstructure formation, because they cannot describe the dynamic nature of the solid–liquid phase transformation. The stochastic nature of the solidification process causes different growth morphologies and the variation in grain size [150]. Numerous models for the simulation of dendritic solidification with cellular automaton-based methods (CA) have been published in the last two decades. A large variety of different concepts have been investigated, an important fraction of them with the intent to reduce the anisotropic influence of the frequently employed Cartesian grid structure [151–154,145,155,156]. These techniques allow reproduction of the grain morphology at the meso-scale up to the scale of the casting. An important distinction should be drawn between microstructure prediction as a post processing exercise and a real-time microstructure-based constitutive behaviour, which potentially comes with a big computational penalty. Stochastic models offer a promising route for linking models of different types of physics at different size scales.

The CA technique was coupled with FE heat flow equations (CAFE) to predict grain structures in castings [157]. Using CA in combination with FD (CAFD) Jarvis et al. could predict the development of a 2D dendritic structure including a macrosegregation profile [158].

### 2.4.2. Phase-field modelling

In the development of models at the dendritic level significant progress has been made in particular by means of the application of the phase-field (PF) method [159–163].

<sup>2</sup> ALSIM is a casting-simulation software package developed by the Norwegian Institute for Energy Technology (IFE), Kjeller, Norway

<sup>3</sup> ABAQUS is a trademark of Dassault Systems Inc., Providence, RI.

A phase-field model (PF) is a mathematical model for solving interfacial problems. In this approach, the sharp boundary between the phases is approximated with a diffuse interface by introducing a PF, a continuous variable, which is constant in the bulk of the phases and varies across the thin boundary layer between them. The method does not require explicit tracking of the interfaces between the phases, which turns out to be, considering the numerical implementation, a huge advantage in comparison to sharp-interface models [164]. The PF models are linked to thermodynamics through the free-energy functional, depending on the PF and other relevant variables, e.g., temperature and solute concentration. Minimization of the free-energy functional yields a set of non-linear partial differential equations governing the evolution of the interfaces between the phases and the transport of heat and mass.

Phase-field models have mainly been applied to solidification dynamics. Phase-field models are usually constructed in order to reproduce a given interfacial dynamics. For instance, in solidification problems the front dynamics is given by a diffusion equation for either concentration or temperature in the bulk and some boundary conditions at the interface (a local equilibrium condition and a conservation law), which constitutes the sharp interface model.

Applying the phase-field technique the growth of a 3D dendritic could be simulated [165]. The method has been applied to a variety of casting phenomena including solute driven isothermal dendritic growth in alloys and coarsening of liquid–solid mixtures in the mushy zone. A recent review by Tourret et al. [166] compared phase field and two newer models, needle based (DNN) and envelope based (GEM) for dendrite growth. They concluded that the two new methods look promising and will help improve the predictive capabilities of mesoscopic models but there is further research to be carried out which if successful will help in extending their use across wider time and length scales than phase field.

Wang and Li [167] concluded in 2010 that despite the huge potential of these PF methods they have yet to prove their value in predicting defects and deformation. Li et al. [168] concluded that PF modelling was still largely qualitative in the prediction of microstructures. A novel Phase-field-crystal (PFC) methodology has recently been developed incorporating solid- liquid and gas phase interactions to qualitatively demonstrate shrinkage in cast binary alloys has been by Wang et al. [169].

Atomistic modelling such as Molecular Dynamics (MD) is another interesting deterministic method that is growing in interest but brings with it very high computation al penalties. Nevertheless with ever increasing computation power the results are starting to become interesting. Fujinaga and Shibuta showed its application to nucleation from grain refiner in aluminium alloys showing how it could demonstrate differences in the growth behaviour dependant on the angle of cavities on the surface of the nucleant [170]. Papanikolaou et al. have recently demonstrated the use of MD in quantitatively predicting residual stresses in solidifying cast aluminium [171].

Despite the research effort over the last two decades in these CA, PF and MD methods the authors believe that they still only produce qualitative results and thus predicting actual locations of real defects in cast shapes is still some way off.

### 3. Modelling of casting defects

Defects common to both processes are dealt with in the next section after which the defects specific to the individual processes are reviewed.

#### 3.1. Defects common to both processes

##### 3.1.1. Cold shuts and surface segregation

**3.1.1.1. DC casting.** During DC casting cold shuts occur by solidification of the meniscus, shrinkage and pull away of the solid away from the mould. Figs. 4 and 5 show examples of cold shuts. [172]

The surface appears to consist of a rather coarse lapping pattern. [173]. Cold shuts can require extra scalping and can also cause hot cracking. Often this cracking is on the rolling face, but it can also occur at the ingot corners. Cold shuts can either occur at the butt of the ingot or over the full contour of the ingot.

Most possible causes for cold shuts are:

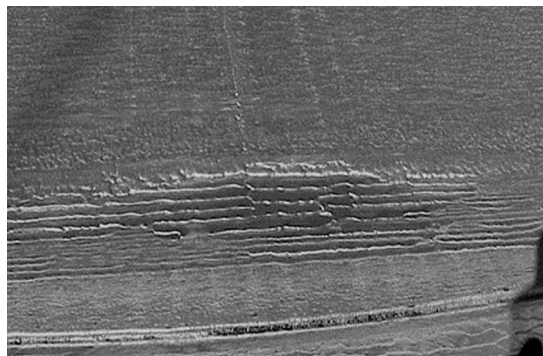


Fig. 4. Cold shuts near start of cast in transition zone [172].

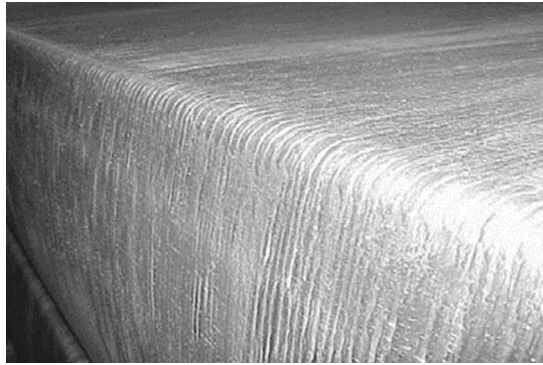


Fig. 5. Cold shuts on ingot corner and edge [172].

- excessive use of mould lubricant
- too much cooling in the mould
- curl of the ingot butt at the start of the cast.

When excessive mould lubricant is the cause, the solution may be to minimise oil flow over the entire mould area. In addition cold shuts are generally caused by too high cooling and/or by a too low casting speed. Raising the casting temperature and/or increasing the casting speed in general should correct the problem. Too much butt curl at the start of a cast can be reduced by casting parameter changes as starting temperature, ramps in water flow, pulsed water flow, CO<sub>2</sub> dissolved in water, fibreglass strips applied to the mould and starting block before the cast, etc. Also at the start of the casting increased ramping to the casting speed should eliminate cold shuts at the butt.

Weckmann and Niessen [174,175] applied a steady-state numerical model and were able to calculate the mould heat transfer coefficient. Formation of cold shuts and folds is controlled by the mould heat transfer, casting speed and refractory overhang. An increased mould heat transfer coefficient facilitates the solidification front to extend deeper into the ingot resulting in larger cold folds. From the calculated mould heat transfer coefficient a critical casting speed could be identified. If the actual casting speed is greater than a critical speed, cold shuts will not be generated. Alternatively, the critical casting speed can be lowered, and cold shuts eliminated, if the mould temperature is increased, the heat-transfer coefficient in the mould is reduced, or the liquid metal superheat is substantially increased.

Surface formation, segregation and exudation during DC casting is described by Bergmann [173] and Buxmann [176] resulting in a typical banded surface structure (Fig. 6).

Mo [177] developed a mathematical model for the development of the segregated layer. The model takes into account the mushy zone flow to the surface. This flow is affected by the periodic movement of the meniscus in the mould whereby the heat transfer coefficient in the mould and the metallic pressure is changing. These phenomena and mechanisms were confirmed by Benum et al. [178] (Fig. 7). Cold shuts or folding occurs when the meniscus solidifies due to too much heat flow in the mould. As the solid metal shrinks away molten metal floods into the cavity. This process repeats until the temperature in the mould becomes hotter.

The 1D model was later extended into a 2D model for sheet ingots [179] and into a 2D for extrusion ingots [180].

These modelling calculations confirmed again that the metallostatic head is the driving force for exudation through the dendritic network. From resulting fluid flow through this network the dynamic thickness of the exuded layer can be calculated. Measurements from two different alloys, with rather small changes in composition, but with large variations on surface quality, compared well with the modelling results [180].

**3.1.1.2. Shape casting.** Cold shuts, cold laps or weld lines are created in shape castings when two metal surfaces meet. They may both be liquid or one may be solid but in both cases there is not enough energy to weld the two metal masses together [181]. Cao et al. [182] have developed a solver that considers the solid fraction, velocity, and volume fraction of the metal phase. The solver predicts the confluence of liquid metal fronts and the subsequent creation of cold shuts using the open source CFD code OpenFOAM.

### 3.1.2. Gas blows and pin holes

**3.1.2.1. DC casting.** Pin-holes or other types of subsurface porosity may not cause ingot cracking, but will require extra scalping. If this porosity is not removed, it can cause slivers or blisters in the rolled products. These can be caused by excessive lubrication, or by excessive steam at mould metal interface.

**3.1.2.2. Shape casting.** Identifying the mechanisms and modelling the occurrence of gas blows and pin holes defects in castings is complex. In shape castings the provenance of the gases causing these defects are most likely to come from polymer binders in the resins used to make sand moulds and cores (mould /metal reaction), burn off of polymers used in coatings or evaporation of water from



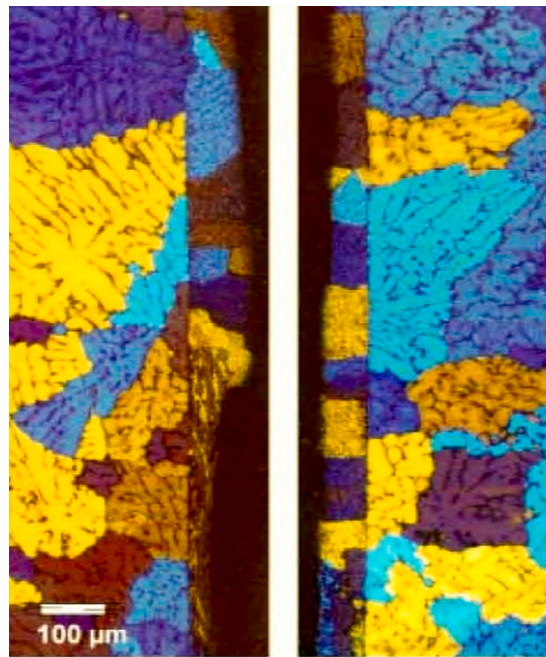


Fig. 6. Typical zone structure of an AA3xxx alloy [178].

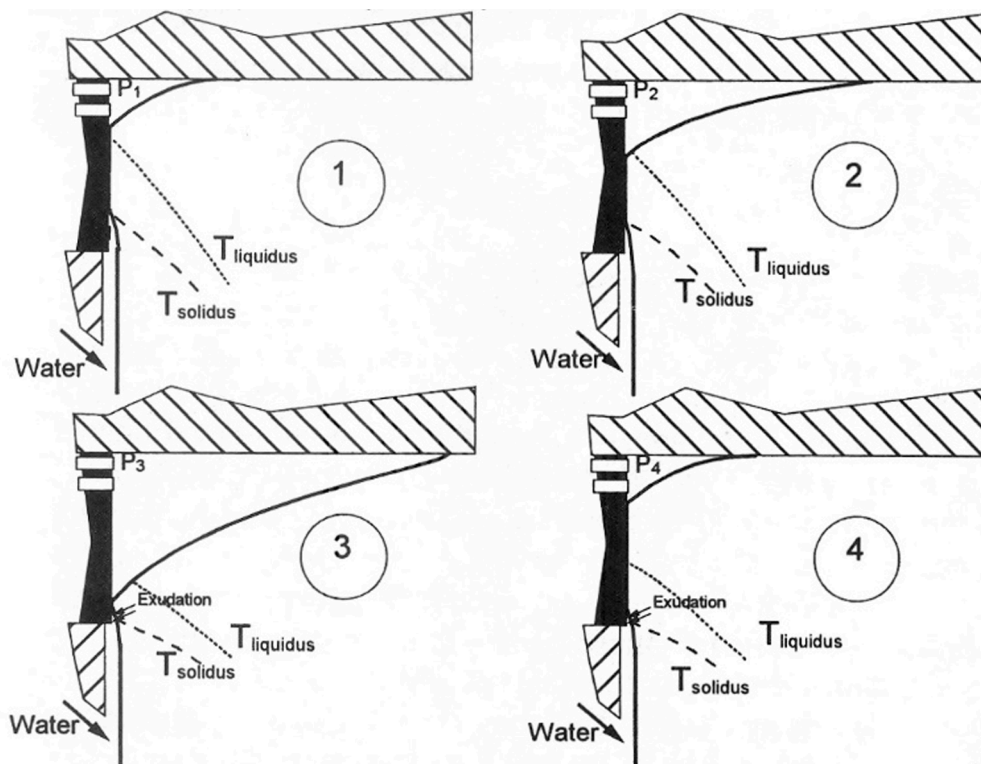


Fig. 7. Formation cycle of periodic segregation [178].

coatings used on moulds and dies. To directly model these events would require a model of the chemical reactions and chemistry of the constituents in each case and is not practicable. Bhone has attempted to categorise these defects in sand casting [183].

### 3.1.3. Casting dimensions and distortion

**3.1.3.1. Shape casting.** Prediction of distortion or shape is extremely important, as this can actually influence the thermal patterns in the casting and hence the final microstructure or porosity. Modelling the gap formation between the casting and mould has been achieved by a number of software packages (Fig. 8).

Modelling of shape change in aluminium castings has been demonstrated by a number of authors. A comprehensive review of the thermomechanical behaviour and modelling of stress, distortion and hot tearing was completed in 2007 by Bellet and Thomas [185] and although all the examples are Fe based the methods can be applied to aluminium alloys. Residual stresses and distortion have been carried out by a number of researchers for a number of casting processes [186–188] (Fig. 9) (Fig. 10).

**3.1.3.2. DC casting.** Before rolling of aluminium sheet ingots the rolling faces should be flat and parallel. Usually this is achieved by scalping of the ingot. To minimise the scalping depth a nearly rectangular cross section of the cast ingot is required. By combining experimental results with a dimensional analysis a model for the prediction of rolling face pull-in was developed [189]. With this model the optimal mould shape for steady state conditions could be calculated. From these experiences a numerical model was developed including calculations of the temperature, stress and strain fields [190]. From the model calculations an almost linear dependency of the pull-in with casting speed could be explained.

Thermal gradients are generated during DC casting due to the difference in cooling rates at surface and centre of the ingot. The surface cools rapidly by the direct contact from the water spray while the centre of the ingot is cooled more slowly. The strong thermal gradients in the ingot may lead to distortion of the ingot shape (e.g. butt curl, butt swell, rolling face pull-in) and eventually may cause hot tearing or cold cracking [7,53,191]. In round billets, normal stresses are mainly compressive at the surface and tensile in the centre [53]. In sheet ingots (slabs) however, the stress state might be slightly more complicated depending on the width to thickness ratio. General speaking, normal stresses appear to be compressive on the rolling face and tensile in the interior [192].

Butt swell (Fig. 11) refers to the thicker bottom of the ingot. Due to a lower casting speed and cooling via the bottom block the lateral contraction is minimal and the ingot keeps the dimensions of the mould. Unfortunately it requires that the butt is removed before further processing [193]. Butt curl (Fig. 11) occurs because the heat transfer is much higher during the start-up phase than during the steady state phase of the casting. Due to the combined excessive cooling by the mould, the bottom block and the secondary cooling, the butt strongly contracts and the ingot curls upwards. This causes several problems: the stability of the ingot on the bottom block is decreased, the thermal contact with the bottom block is reduced and hot tears may form [53,193,194].

During the steady-state phase of the casting process, thermal contraction and solidification shrinkage cause a strong pull-in (up to 10%) of the rolling face. This may lead to a ‘bone-shaped’ ingot cross-section. This problem is solved by using a convex mould, which leaves a rectangular ingot after casting.

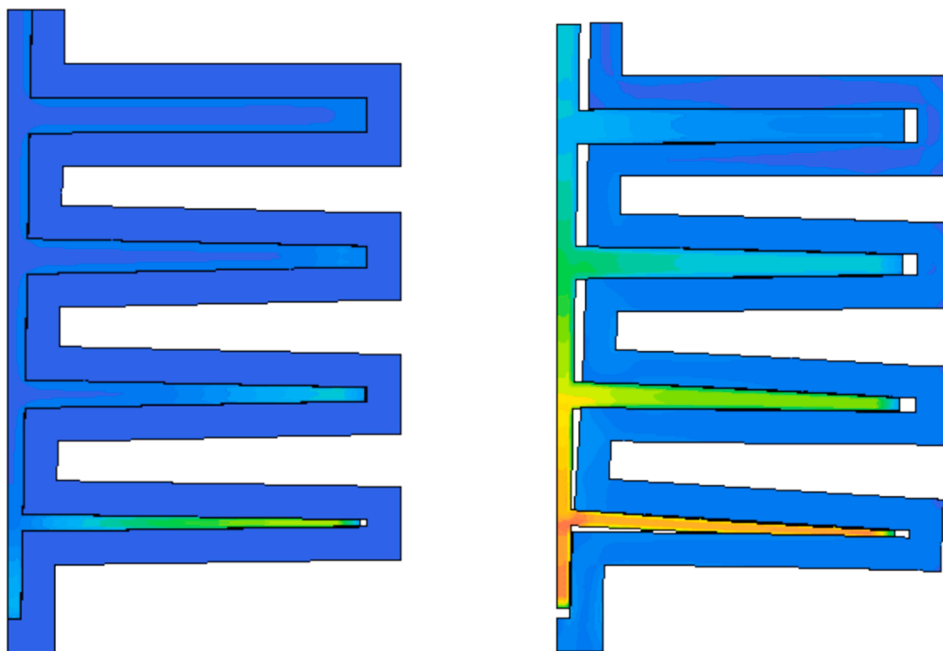


Fig. 8. Development of air gap in 3D model of investment casting solidification [184].

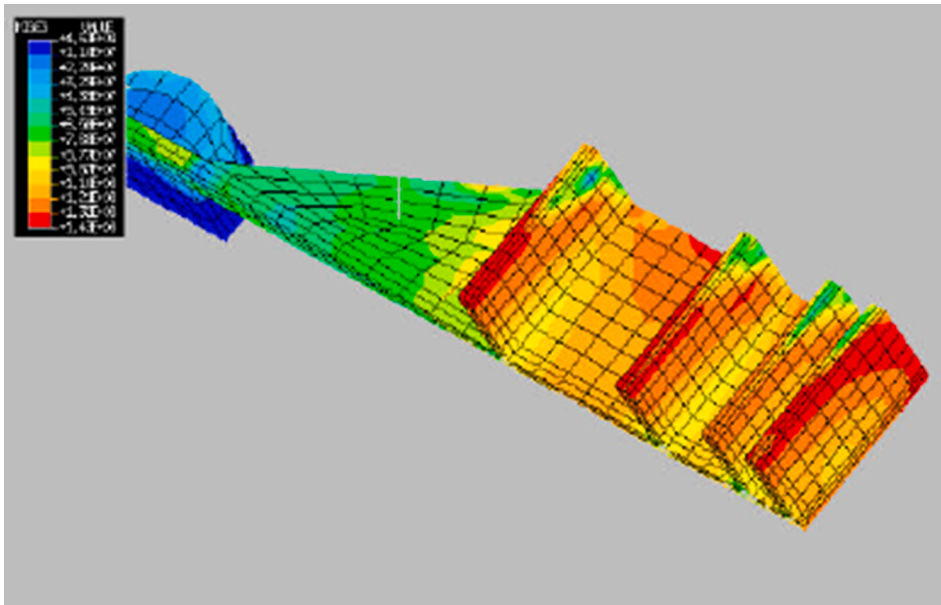


Fig. 9. Residual stresses in high pressure die cast A380 alloy casting at ejection – elasto-plastic model [187].

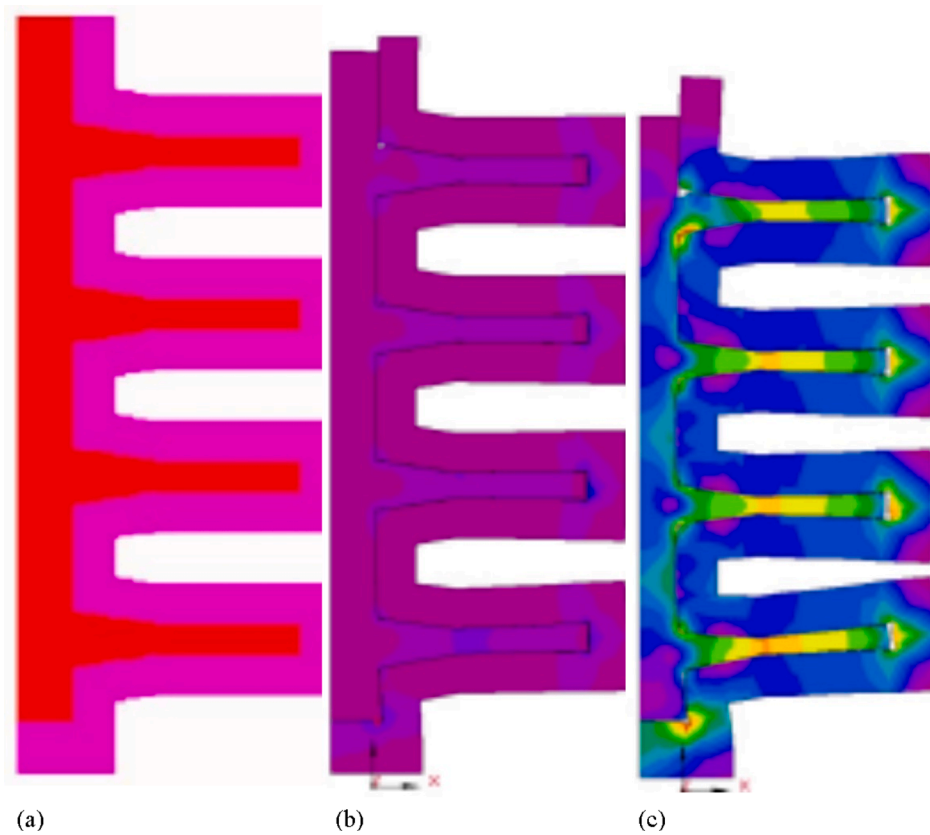


Fig. 10. Stress development in an investment casting using 2D finite element analysis: (a) liquid metal in shell; (b) start of solidification; and (c) end of solidification [117].

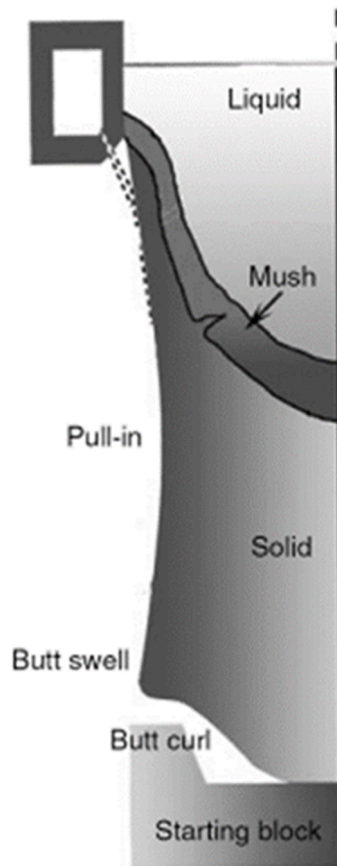


Fig. 11. View from the short side of the ingot showing distortions typical of DC cast ingots [6].

Drezet and Rappaz [191] developed comprehensive three-dimensional (3-D) mathematical model based upon the ABAQUS software for the computation of the thermomechanical state of the solidifying strand during DC casting of rolling sheet ingots and during subsequent cooling. Based upon a finite element formulation, the model determines the temperature distribution, the stresses, and the associated deformations in the metal. The 3-D thermomechanical model has been validated using ingot distortion measurements and is able to predict with accuracy the butt curl of the ingot during the starting phase and the transient and steady state rolling faces pull-in as a function of the casting conditions (casting speed, ingot size, and mould shape).

#### 3.1.4. Hot tearing/hot cracking

**3.1.4.1. Shape casting.** Propensity for hot tearing in shape casting has been inferred, as Fig. 12 illustrates, although this is only currently possible by interpretation of the data. Models for hot tearing exist for DC casting but have yet to be incorporated into shape casting simulations. Much research has been carried out in this area examples are given in [195–197] Shyam et al. [198] investigated a number of defects including hot tearing in A319, A356 and A206 alloys using an integrated computational materials engineering (ICME) approach to determine the performance of the alloys for a complex cylinder head casting. Sabau used a similar approach to predict mechanical properties based on calculated or measured values of both microstructure and porosity defects [199]. Recently Chen et al. [200] coupled a phase-field model and CFD to predict hot cracking. With the inclusion of the columnar to equiaxed transition it was found with the associated pressure drop equiaxed grains have a great impact on the liquid feeding.

**3.1.4.2. Hot tearing during DC-Casting.** The mushy zone, where solidification takes place, can be divided into several parts. At the *coherency temperature* solid grains start interacting and the viscosity increases sharply. The metal behaves as a slurry and can be described by viscosity models [201]. The *rigidity temperature* marks the formation of the continuous network of solid grains. The dendritic network can transfer stress [202] and as a result behaves as a solid.

DC casting cracks can be divided into hot tears or hot cracks occurring in the mushy zone above the solidus [203], and cold cracks forming in the solid. Hot tears are frequently observed in the centre of the ingots/billets where high tensile stresses arise (Fig. 13) but they can also appear at the surface. Surface cracks are hot cracks that are formed due to air gap formation [6]. Cold cracks in the fully solidified material occur mainly in the high strength alloys (2xxx and 7xxx alloys) and are due to thermal stresses built up during

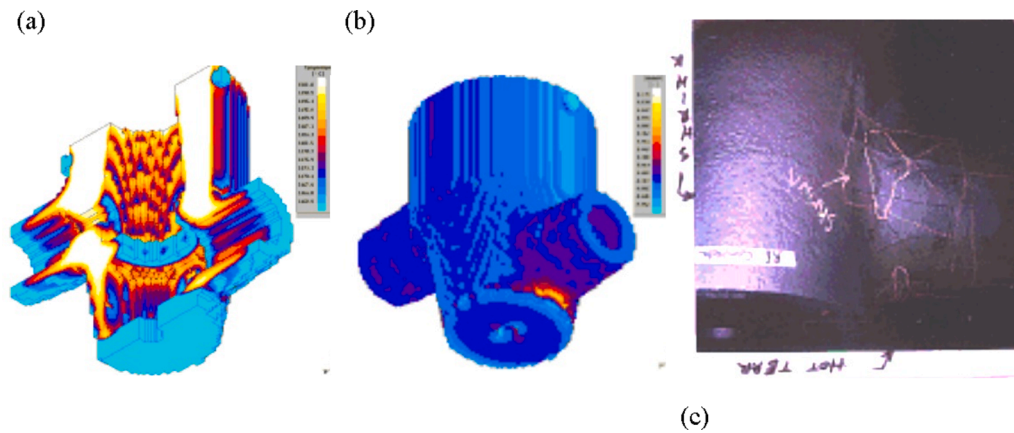


**Fig. 12.** Representation of hot tearing in the MAGMAsoft code: (a) the isotherms on solidification; (b) the surface stress concentrations (lighter area); and (c) a photo of the casting surface itself, taken by the foundry [117].

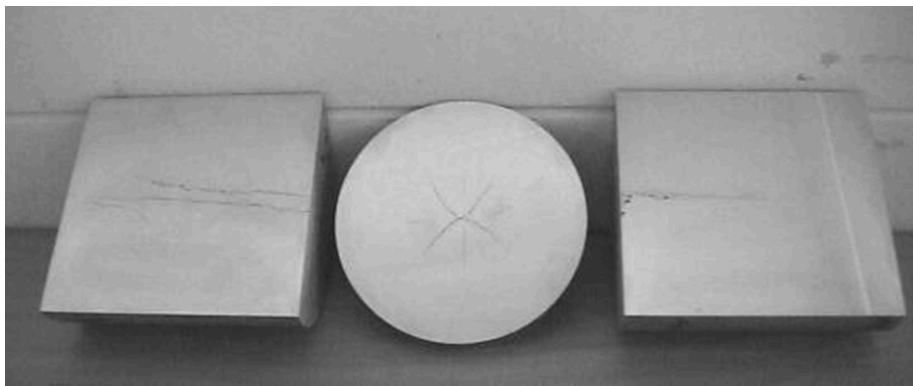


**Fig. 13.** Photograph showing hot tears in the centre of 200-mm radius Al-Cu billets [206].

casting and subsequent cooling to room temperature [53,204] Cold cracking will be discussed in Section 3.2.2.

Numerical simulation of thermal stresses during DC-casting have been applied to predict the occurrence of hot cracks [191,205], or cold cracks [192].

The main factors for hot tearing are well understood [7]. Initially, liquid feeding becomes insufficient and micro-pores are formed. The solidification shrinkage and thermal contraction will impose stresses and strains on the semi-solid network. Fracture occurs in the liquid film surrounding the solid grains, when the stress exceeds the tensile strength of the material. The fracture surface is covered with a liquid layer and sometimes solid bridges [205]. Finally the microstructural evolution and precipitation of secondary phases during solidification will also effect the hot tearing susceptibility [207].

Hot tears often occur during the start-up phase of DC casting. Initially the cooling in the centre of the ingot is delayed, which results in an overshoot of the pool depth before reaches steady state. Two methods are applied to prevent hot tears to initiate at the start-up [208]:

- ramp the casting speed up to the desired speed
- raise the central section in the starting head [209,210]

M'hamdi et al. [63] investigated the effect of different initial casting speeds on the thermomechanical and hot tearing behaviour in a DC-casting of an AA6060 alloy using a simplified visco-plastic equation [211]. The calculated visco-plastic strain rate corresponds well with the measured hot tearing susceptibility. Applying Eq. (3), Suyitno et al. [62,212] calculated the effect of start-up practise on the thermo-mechanical and hot tearing behaviour in a DC-casting 200-mm Al-4.5 wt% Cu alloy round billet. When the sump depth at the centre of the billet becomes wider, the thermal gradient between the centre and surface of the billet will increase, which leads to higher tensile stresses and strains. The slowest start-up mode produces moderate stresses and strains as well as the minimum sump depth and mushy zone length, which results in a minimum hot cracking susceptibility.

Modelling of hot tearing during DC casting is accomplished in two steps. In the first step constitutive equations (see Section 3.1.4.2) are used in the thermomechanical modelling to calculate stresses and strains [75,213]. In the second step the computed temperature

and stress fields are used as input in a hot tearing criterion [205] (see also Section 3.1.4.2.1).

**3.1.4.2.1. Hot tearing criteria.** Over the years many hot tearing criteria have been proposed. These criteria can be classified into two categories: mechanical and non-mechanical. The mechanical criteria are either based on critical stress, critical strain, or critical strain rate. The non-mechanical criteria contain vulnerable temperature zone, phase diagram, and process parameters. Eskin et al. [205] have reviewed these criteria in 2004 and their applicability. More recently new hot tearing criteria have been formulated, of which most relevant are discussed below.

**SKK criterion**

Suyitno et al. [212] proposed a hot tearing criterion based on micro porosity formation. In this so called SKK criterion, several phenomena are considered. When the coherency temperature is reached and a coherent dendritic network is formed the remaining liquid becomes isolated and porosities may form at grain boundaries due to solidification shrinkage, thermal contraction, and low permeability [6].

Three possible phenomena may occur in the last solidification stage.

- The liquid flow and shrinkage flow fully compensate for the solidification shrinkage and thermal contraction and no cavities are formed
- Feeding possibilities are limited and the pores are formed
- When the pore size  $d$  exceeds a critical size  $a_{\text{crit}}$ , hot tearing will occur.

The  $a_{\text{crit}}$  is determined by using the modified Griffith criterion:

$$a_{\text{crit}} = 4\gamma_1 \frac{E}{\pi\sigma^2} \quad (8)$$

$\gamma_1$  is the surface energy of the liquid phase;  $E$  is the Young's modulus of the semi-solid;  $\sigma$  the tensile stress.

The hot tearing susceptibility (HTS) is defined as:

$$HTS = \frac{d}{a_{\text{crit}}} \quad (9)$$

When  $HTS > 1$  hot tears may occur. The SKK criterion correctly predicts the effects of deformation rate, cooling rate, grain size, casting speed, and casting recipe [212]. The SKK criterion was successfully applied to predict the compositional sensitivity of hot tearing in grain-refined Al-Mg-Zn-Cu alloys using the measured load developments upon solidification [82]. However the prediction of an increasing hot tearing tendency with a high value at the solidus temperature does not agree with casting practice. The SKK model incorrectly assumes that all grains are surrounded by a liquid film. However, microstructural observations clearly indicate that grain bridges are formed at the last stages of solidification. Bai et al. [214] improved this criterion by including the effect of solid bridging and grain coalescence. Two additional parameters were hereby introduced into the criterion, including the fraction of grain boundaries covered by liquid and a solid energy term ( $U_s$ ), representing the activation energy required for hot tear propagation along the grain boundaries. The critical cavity size is now formulated as follows:

$$a_{\text{crit}} = 4[\gamma f_{\text{LGB}} + U_s(1 - f_{\text{LGB}})] \frac{E}{\pi\sigma^2} \quad (10)$$

$f_{\text{LGB}}$  is derived in a similar way according to Wray's treatment [66] as discussed in Section 1.5.3.1. This modified criterion responds well to the change in the deformation rate, cooling rate, grain morphology and casting speed [214]. The evolution of critical stresses obtained with the modified criterion is clearly different from the result from the original SKK criterion, which will lead to a decreased hot tearing tendency close to the solidus, which is in agreement with the industrial practice.

**Two-phase model**

The Tearsim two-phase model was suggested by M'Hamdi et al. [215]. In this strain-based criterion, the initiation and propagation of pores due to the lack of feeding at the last stage of solidification and the localization of visco-plastic deformation is regarded as the main cause for hot tearing. The effective strain of the dendritic network is considered as the hot tearing indicator. Above the critical strain, hot tears will form. The value of the critical strain depends on microstructure, number of pores, dendritic coalescence, distribution of liquid films, and the wetting conditions [215]. Tearsim has been successfully applied to predict hot tears under different DC casting process parameters, including casting speed and its ramping rate, grain refinement, and kind of starting block [215].

**3D Granular model**

This model couples granular mechanics with the thermomechanical behaviour of solidifying alloys and consists of four separate modules [216]:

- a solidification module to calculate the liquid–solid geometry at a given solid fraction
- a fluid flow module to calculate the liquid pressure drop
- a semi-solid deformation module for the rheological behaviour of the granular structure; a failure module for crack initiation and propagation

The hot tearing criterion used in the granular model is an extension of the RDG criterion [217]. The granular model was successfully applied to predict hot tearing observed during X-ray micro tomography [218]. The formation of hot tearing in grain

boundaries is modelled including stochastic variations in grain morphology and DC casting process parameters [219].

3.1.4.2.2. *Application of hot tearing criteria.* Suyitno et al. [62,212] have systematically evaluated the process parameters sensitivity of several commonly-used hot tearing criteria by implementing them into a thermomechanical model of DC casting. Most criteria predict that a high casting speed leads to higher susceptibility to hot tearing in the centre of the round-shaped billet, in agreement with casting practice. But these criteria do not include ramping of the casting speed during the start-up except the criteria proposed by Rappaz et al. [217] and Suyitno et al. [212]. Only the SKK criterion responds correctly to all relevant casting parameters. Bai et al. [214] modified the SKK criterion and the improved SKK criterion is in better agreement with DC casting practice. The effective application of the SKK and modified SKK criterion is dependent on the availability of properties such as Young's modulus of the mush, the surface tension between the solid phase and liquid phase, the fraction of grain boundaries covered by liquid. These properties are limited and need to be measured.

### 3.1.5. Porosity

During the last stage of casting porosity may occur in aluminium castings due to the shrinkage upon solidification. The presence of porosities largely affects the mechanical properties of cast products. Rappaz [220] recently reviewed investigations in which solidification micro models were included.

3.1.5.1. *Shape casting.* Casting simulation initially started with the prediction of solidification shrinkage, since this was perceived as being the most prevalent casting problem. Primary shrinkage is now well understood and it is probably one of the most accurately predicted of all the defects found in consideration of the local conditions of temperature and cooling rate. One such function, the Niyama criterion, is used for short freezing range alloys and especially steels, and utilizes the relationship between the temperature gradient,  $G$ , and the cooling rate,  $R$ :

$$\text{Niyama criterion} : G/(\sqrt{R}) \quad (11)$$

A plot is then made of the regions within the casting where the value of the criterion function chosen is greater or less than a specific value which is dependent on the alloy system being cast (Fig. 14).

A review of some of these criteria functions has been written by Taylor et al., [221]. What is often valuable to the cast metals engineer is to be able to predict the order of solidification of the various parts of the casting. This can be represented in many ways: as isothermals, isochronals, or liquid/mush/solid, for example.

Representation of porosity has always led to an interesting debate. Some software packages represent the porosity as the probability of porosity contours, others as discrete "holes" in the casting geometry. Some software packages can also show different levels of porosity, depending on what quality level the operator dials in. Fig. 15 illustrates some of the ways in which porosity is represented.

Porosity in shape casting is often a combination of shrinkage porosity and hydrogen porosity. A number of researchers have proposed models for predicting hydrogen porosity [222,223]. Gu and Luo [224] have developed a model that combines the effects of shrinkage pressure and initial hydrogen content on porosity evolution and final porosity percentage which are then related to location-specific microstructure in cast aluminium. A multiphase-field model was developed to simulate the evolution of both solid phase and hydrogen pore during solidification in a binary Al-Cu alloy [225]. The driving forces for the solid-liquid and liquid-gas transitions are the undercooling and pressure difference respectively. Results show that the presence of hydrogen pores substantially changes the dendrite network.

3.1.5.2. *DC casting.* Lee et al. [226] developed a model to predict the formation of porosity during the DC casting of Al – Mg alloys. The porosity model was incorporated as a post-processor to a commercial transient macro model of the three-dimensional heat transfer and fluid flow. The porosity model not only predicts the percentage porosity, but also the size, shape and distribution of the pores. The sensitivity of the model to process and alloy variations was evaluated, showing the importance of the cooling rate and hydrogen concentration. An experimental study of the amount of porosity in laboratory scale (250 × 400 mm cross-section) DC cast ingots of Al 2, 4 and 6 wt% Mg was performed. The results from these experimental billets were used to validate the model as a function of the location in the ingot and the initial hydrogen and magnesium content. The model correctly predicted the experimentally observed trends, showing good correlation to the measured percentage porosity. M'Hamdi and Mo [227] extended an existing two-phase mathematical model that addresses hot tearing formation in aluminium castings to include microporosity formation. An application addressing the start-up phase of aluminium direct-chill casting reveals that thermally induced deformations increase the porosity level.

### 3.1.6. Microstructure

3.1.6.1. *Shape casting.* The routine simulation and prediction of microstructure is fast becoming a reality [15]. Predictions of grain size, growth, and orientation are being carried out at larger organizations and research establishments, but these are still not commonplace in most shape casting companies. Modelling of grain structure in an ingot is now possible (Fig. 16). Individual dendrite growth can also be modelled well now using either CA [158] or phase field techniques [159,165]. However, there is some way to go before this can be carried out on a full-size casting, as the CPU required for discretization at that level would be enormous. Voller [228,229] predicted that with the rates of improvement in hardware and software, it would still take until 2040 to be able to model dendrite tips in a casting space envelope of 10 cm × 10 cm × 10 cm.

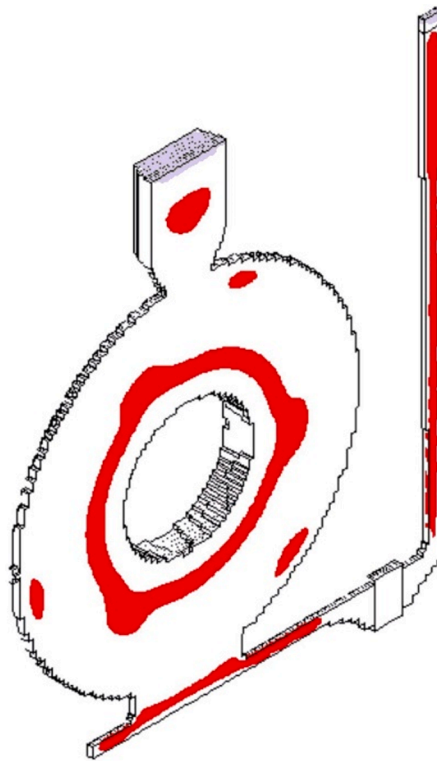


Fig. 14. Plot of the Niyama criteria = 0.8 for that section of the casting [117].

**3.1.6.2. DC casting.** Microstructural modelling in DC casting is largely concentrated around the prediction of grain sizes and the effect of grain refiners. Rappaz et al. [231] were the first to propose a multiscale diffusion model to numerically simulate equiaxed dendritic solidification in castings accounting for grain morphology. Based on this approach Hakonsen et al. [232] developed a micro/macro model for dendritic equiaxed grain nucleation and growth during DC casting of sheet ingots. Different nucleation laws, which all relates the nucleation to the undercooling of the melt, were compared. The results of the micro model are the evolution of the solid fraction until impingement of the grains, the distribution of the alloying elements, as well as the mean grain size versus position in the ingot. The macro model for heat and fluid is coupled with the micro model by an iterative micro/macro time step scheme. This coupling makes it possible to calculate the grain size distribution versus position in the ingot. The modelling results compared well with measurements of secondary dendrite arm spacing and mean grain size in ingots with varying grain refiner additions. This modelling approach was further extended by Bedel et al. [233] in which the coupling between nucleation and growth of the grains in presence of liquid convection at the macroscopic scale was included.

To further improve the prediction of hot cracking an integrated 2D model of coupling phase-field model together with CFD calculations was proposed [234]. In this approach columnar dendrites with different orientation angles, different grain sizes of equiaxed grains, and columnar to equiaxed transition (CET) were simulated. The RDG model [217] was used to evaluate the hot tearing susceptibility (HTS) of these simulated microstructure features. The simulations have shown that the feeding pressure drop varies as a function of grain orientation, while it remains constant in the RDG model. As a result equiaxed crystals with large grain sizes have a higher HTS due to their large pressure drop as well as a narrow liquid channel.

## 3.2. Defects specific to DC cast ingots

### 3.2.1. Macrosegregation

**3.2.1.1. Physics.** The main mechanism behind macrosegregation is well understood: the relative movement of liquid and solid phases [235,6,236], which can be caused by several effects:

- Buoyancy driven flow, which is caused by concentration (solutal convection) and thermal gradients (natural convection) in the melt
- flow that fills the cavities formed by solidification shrinkage
- transport of the floating grains, which are formed at the beginning of solidification and are free to move



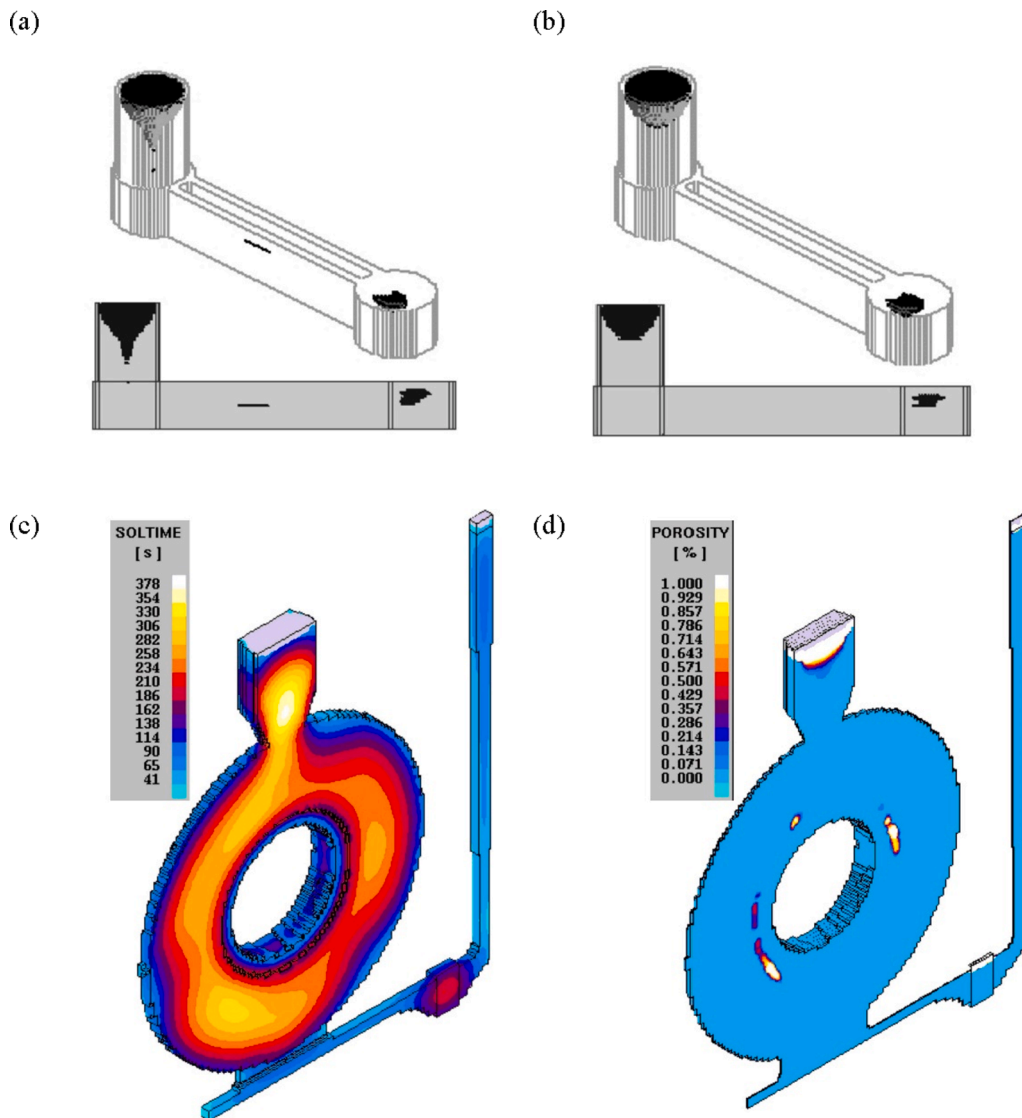


**Fig. 15.** Selection of representations of solidification results: (a) and (b) show porosity the way that X-rays would, but in both 2D and 3D and for two different quality levels in the same casting; (a) shows higher-quality level defects than (b); (c) solidification time contours (isochronals); (d) shows porosity contours: blue is sound, white is a pore, and the other colours are probabilities that porosity will occur [117].

- flow driven by the deformation of the dendritic network due to thermal contractions or mechanical treatment of the billet outer shell

Additionally, the macrosegregation evolution can also be affected by a range of factors including forced flow, induced by pouring, mechanical or electromagnetic stirring, ultrasonic melt processing, vibration and rotation. In particular metal entry systems into the mould can have a major influence on macrosegregation levels [237]. Buoyancy driven flows, like natural convection, largely depend on the dimensions of the liquid sump<sup>4</sup>. High casting speeds and large ingots cross sections create deep sumps resulting in more macrosegregation [238].

**3.2.1.2. Model description.** Macrosegregation models are single domain methods, based on either volume averaging technique [147,146] or mixing theory [239]. These one-phase single domain or multiphase single domain models, originally formulated by

<sup>4</sup> Natural convection can be characterised by either the dimensionless Grashof number, the ratio of inertial and viscous forces or the Rayleigh number, the ratio of gravitational and viscous forces. Grashof and Rayleigh number both depend on the sump depth to the cubic power. Both numbers are related according  $Ra = Pr \cdot Gr$  in which  $Pr$  is the Prandtl number, the ratio of kinematic viscosity to the thermal diffusivity



Fig. 16. Grain structure prediction in an Al-Si alloy cast ingot [230].

Bennon and Incropera [239] and re-assessed by Prescott and Incropera [240], are implemented to predict macrosegregation during DC casting of multicomponent alloys. A single domain model was applied to predict macrosegregation in DC cast Al-4.5 wt% Cu billets by Flood et al. [32]. Assuming that the mushy zone consists of a rigid, permeable solid matrix moving at the casting speed, positive segregation of copper was predicted at the centre of the billet. For the one-phase single domain model no interfacial transfer terms are required in the equations. They contain only macroscopic variables, which facilitates the numerical solution. The more detailed description in the multiphase models needs the inter-phase transfer terms to be known. For the application of a single domain model the temperature, composition and velocity of each phase need to be known beforehand. The temperature field in a finite volume is the same for the solid and liquid phase due to the large value of Lewis number<sup>5</sup>. But the compositions and velocities in the two phases have to be determined at a micro scale.

In this case a micro model calculates the fractions of various phases, the temperature, and the liquid composition. A micro model in the context of DC casting must include possible remelting, which can occur in two different ways:

- When the heat transfer coefficient changes dramatically (for example between the primary and secondary cooling, in the air gap)
- When solute-rich liquid is entrained in a region of low alloy concentration in the mushy zone

In order to model the relative movement between solid and liquid in a one-phase single domain macrosegregation model an inter-phase drag model is required. This inter-phase drag depends on grain morphology, grain size, solid fraction, etc. The simplest relationship is the mushy fluid model [241], in which the velocities of solid and liquid phase are equal. However, this approach is too simple, because even at very low solid fractions, there is always relative movement between equiaxed grains and the liquid phase. To overcome this limitation, Ni and Incropera derived an expression to relate the solid velocity of free-floating dendrites to the liquid velocity [242].

Another point arises when the solid fraction is large enough for small equiaxed grains to be packed together, which makes the floating of equiaxed grains impossible while the interdendritic liquid phase can still flow inside the solid network. The rigid network model, in which the solid velocity is prescribed and the interdendritic liquid flow is modelled by the Darcy law [239], can be employed to describe the flow at this stage. The Darcy-type flow is mainly determined by the permeability within the porous network. Krane and Incropera [243] confirmed the applicability of the Darcy law by a scaling analysis.

The extension of macrosegregation models to multicomponent alloys is an essential step to make the model applicable for industrial applications [244–246]. Crucial for the extension is the description of the solidification path for a multicomponent alloy, i.e. a microscopic model relating the specific enthalpy and local average solute concentration variations to the solid fraction, temperature, and solute concentrations in the solid and liquid parts of the two-phase volume elements. Solving the set of equations for multicomponent alloys requires an easy and quick access to phase diagram data. This is achieved by indirect coupling with Thermo-Calc

<sup>5</sup> The Lewis number represents the ratio of thermal diffusivity and diffusion coefficient

[46] or similar software. The so-called mapping technique, has been implemented and successfully applied to describe Al–Mg–Si solidification paths [247]. The information related to each forming solid phase, including its liquidus and partition coefficients, is tabulated into a file, and a specific phase diagram module is provided to deduce equilibrium phase fractions and concentrations under a given temperature/composition condition. Once the mapping file is obtained, only a simple interpolation procedure is needed during the main calculation.

Models with different levels of complexity ranging from a linear approximation of the solute profile in the dendrite arms to fully numerical solution of the diffusion equations with moving boundary, have been developed [246,147,248]. The solidification path of a ternary alloy derived with the lever rule has been described in detail in Ref. [245]. The Gulliver–Scheil model formulation is given in Ref. [249].

Numerical models that incorporate the macroscopic transports with microscopic relations for grain growth and solutal undercooling have also been established [37,250]. Partial verification of a finite-volume model for macrosegregation was carried out Zaloznik et al. [251]. The accuracy of the solution for the flow field and the thermal convection was found to be satisfactory.

An important aspect in macrosegregation modelling is numerical dispersion and diffusion in the predicted macrosegregation profiles. Venneker and Katgerman [252] discussed the numerical diffusion introduced by discretisation schemes and it was concluded that the numerical diffusion could be avoided by aligning the mesh with the flow field. Later they tested different numerical schemes [253] and determined that numerical predictions can be improved not only by decreasing the computational cell size, but also with the correct choice of the discretisation scheme. Du et al. [254] concluded that the best solution to minimise numerical dispersion was to employ a hybrid mesh combining structured and unstructured meshes.

A multi-physics DC casting models, based on the meshless approach, have been recently developed with the capability to model macrosegregation [255]. The meshless model, used for industrial applications, has been verified with benchmark cases. The results show a very good agreement with the classical finite volume method and the meshless local radial basis function collocation method. The simulations are performed on uniform and non-uniform node arrangements and it is shown that the effect of non-uniformity of the node distribution on the final segregation pattern is almost negligible [256].

Most modelling efforts are steady state calculations, and the transient effects like the start-up of DC casting are only recently considered [257,258]. Transient modelling of grain structure and macrosegregation during DC casting was achieved with a cellular automaton (CA)–finite element (FE) model, by which the macroscopic transport is coupled with microscopic relations for grain growth. In the CAFE model, a two-dimensional (2D) axisymmetric description is used for cylindrical geometry, and a Lagrangian representation is employed for both FE and CA calculations. The grain structure and macrosegregation including thermal and solutal convection are studied [259].

**3.2.1.3. Macrosegregation modelling results.** A macrosegregation benchmark for binary alloys was carried by four different numerical codes, employing different numerical methods (FVM and FEM) and various solution schemes. The predictions of the macrosegregation were compared for a small ( $10 \times 6$  cm) ingot of Sn-10 wt%Pb alloys [260]. Considering the transport of free-floating grains, separate and distinct mixture momentum equations were employed for a slurry and a rigid solid matrix by Vreeman et al. [261], and the negative segregation was predicted at the centreline in DC cast Al-4.5 wt% Cu and Al-6.0 wt% Mg billets. A benchmark for the meshless method was carried out by Hatic et al. [262] for a round ingot of a binary Al-4.5 wt%Cu alloy. Results were compared with FVM and were in good agreement.

Using one-phase continuum mixture model, Zaloznik et al. [263] investigated the effects of the billet diameter, casting temperature, casting speed and mould cooling type on the final macrosegregation in DC cast Al-5.25 wt% Cu alloy billets. The model accounts for the thermo-solutal convection and solidification shrinkage.

In Fig. 17 the radial Cu composition profile at the height of 500 mm predicted by Chen et al. [259] is compared with the steady state one calculated by Vreeman et al. [264] in the non-grain-refined billet, in which the solid is assumed as rigid. Both profiles give an overall tendency that the average composition increases toward the centreline, showing a negative segregation near the surface and a

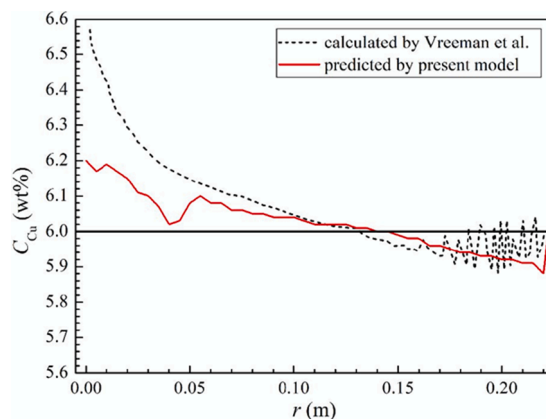


Fig. 17. Radial Cu composition profiles predicted by Chen et al. [259] at the height of 500 mm and calculated by Vreeman et al. [264].

positive segregation near the centreline. However, the predicted profile shows a significantly lower composition near the centreline, and an obvious composition fluctuation is observed near the centreline. As the main difference between the Chen et al. model [259] and the model given by Vreeman et al. [264], the coupling of grain structure and macrosegregation may be responsible for this discrepancy. Also, the predicted profile by Chen et al. [259] is smooth near the surface, while that calculated by Vreeman et al. [264] shows a significant oscillation.

Eskin et al. [265] implemented a multicomponent continuum model and examined the contribution of each solute element to the final segregation pattern in a DC cast Al-Cu-Mg alloy billet. The comparison of the calculated results with experimental values in Fig. 18 shows that, although the qualitative agreement is found in terms of the general segregation pattern and the difference in Mg and Cu segregation, the predicted negative centreline segregation is overestimated.

Many factors could contribute to this overestimation. However, a permeability model is believed to be an important contributor due to the difficulties in measuring the permeability. To get a better agreement with the experimental results, the permeability constant was increased to  $5 \times 10^{-10}$ . An alternative has been suggested by Vreeman et al. [266]; the flow in the range of very low solid fraction is not modelled by the Darcy law but by a simple drag model.

Zaloznik and Sarler [267] showed that thermosolutal flow is an important factor determining the flow configuration in the liquid part of the casting and thus the origin of macrosegregation patterns.

Computer simulations for the Al-5.25 wt% Cu direct-chill cast billet with the meshless numerical model calculated the effect of the casting geometry on melt flow distribution, sump depth, temperature distribution, and macrosegregation [263]. The results show that geometry has a substantial effect on the liquid velocity distribution. A typical macrosegregation pattern for the presented model is positive in the centre and negative at the surface. The strength of the macrosegregation depends on the inlet geometry. The simulation with the simplified inlet design has a less pronounced segregation than the ones performed on more realistic designs. The meshless model is not able to predict the exact macrosegregation pattern in industrial castings, as the thermosolutal flow and the influence of the inlet design are the only phenomena taken into account.

Mostly the simulations for sheet ingot are carried out in 2D. However sheet ingots have an asymmetric geometry in particular with the inclusion of the inlet jet. To avoid this a full scale 3D sheet ingot model with two different inlets was applied by Pakanati et al. [268,269]. A simplified three-phase multiscale solidification model accounting for solidification shrinkage, natural convection and equiaxed grain growth and transport was used to conduct this study [270,271]. The 3D model shows that a different inlet flow geometry affects the grain settling and eventually results in a different macrosegregation pattern. The effect of the inlet geometry on macrosegregation was also demonstrated by Zhang et al. [272].

Semi-quantitative agreement with the experimental data is achieved in macrosegregation calculations which consider both buoyancy driven flows and shrinkage. Better descriptions of the permeability in the mushy zone, grain motion, and surface exudation are needed to get a better agreement with experimental data.

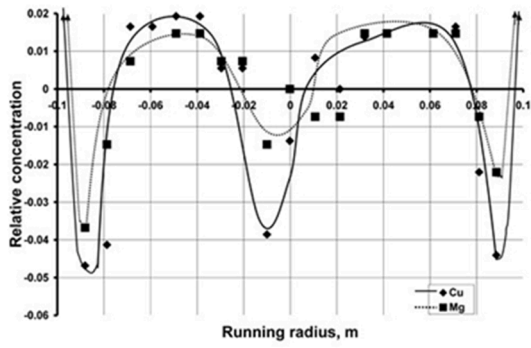
### 3.2.2. Cold cracking during DC casting

The most serious casting defect during in DC-casting of high strength aluminium alloys is cold cracking (Fig. 19). Based on the shape of the crack and the location in the ingot cold cracks are classified as either trouser or J-cracks (Fig. 20). Cold cracks are the result of high thermal stresses in the solid metal and nucleate on defects such as an inclusion or a micro-cavity. Further investigations revealed that the brittleness of the high strength heat treatable alloys (2xxx and 7xxx series) in the as-cast condition facilitates the cracking and failure of the material [273].

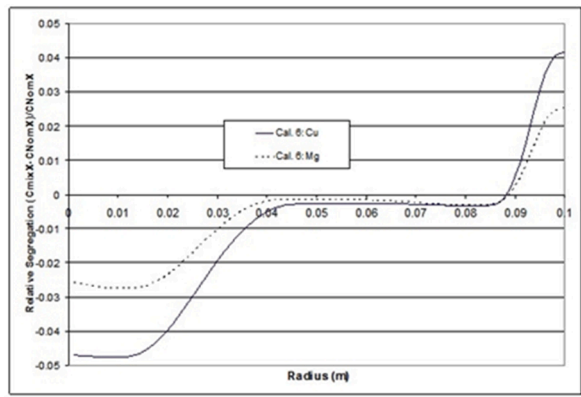
The most efficient way of reducing thermal stresses in the ingots is to reduce the temperature gradients during the DC-casting process [274]. Ingot wipers are designed to control cold cracking by removing coolant from the ingot surface and reducing the temperature gradients below the wiper plane [275] (Fig. 21).

**3.2.2.1. Modelling of cold cracking of DC ingots.** It is not clear whether cold cracks are hot cracks that propagate or cavities reaching a critical size in the presence of a tensile stress field [276]. Criteria developed on cold cracking can be classified in two groups: experiment-based criteria [7], and computer simulation based criteria [277,278]. The disadvantage of experimentally derived criteria is that many casting trials are required to obtain the optimum casting conditions. Computer simulation criteria are based on physical concepts with the inclusion of fracture mechanics. With the right selection of the crack geometry, the critical crack size leading to ingot failure can be calculated. Normal stress values can be obtained through thermo-mechanical simulation of the DC-casting process. Plane strain fracture toughness ( $K_{Ic}$ ) values are required in as-cast condition and need to be established experimentally. Application of the as-cast constitutive parameters, mechanical properties and plane strain fracture toughness ( $K_{Ic}$ ) values can lead to realistic simulation results and eventually reliable critical crack sizes may be assessed [279]. Boender et al. [277] also studied the effect of wipers on the eventual critical crack size and noticed that the cracking probability decreases due to the partial stress relief by the reduced cooling below the wipers.

**3.2.2.2. Thermo-mechanical model.** Mathematical models for the simulation of the combined effects of fluid flow, heat flow and stress generation have been developed since the late 80s [280,12]. In most cases thermal stresses are being calculated with FEM software packages [53,281]. As an example we describe how the dedicated ALSIM5 model [137] is set-up for the computation of temperature profile, stress and strain fields. Rectangular bilinear isoparametric elements with four nodes are used that become finer towards the surface of the billet. As the bottom block moves downwards during casting, new elements are added to the geometry at the casting speed, while mould, hot top and molten metal retain their initial position. Time-dependent thermal boundary conditions are applied to



(a)

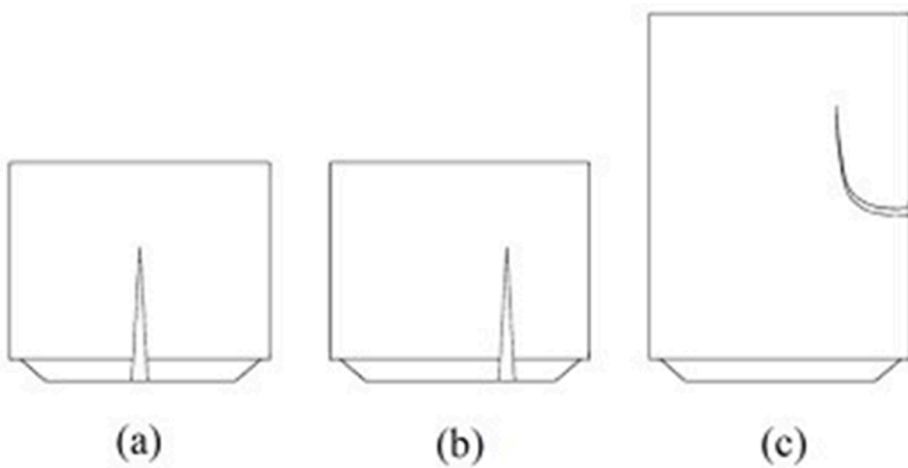


(b)

Fig. 18. Experimentally observed (a) and calculated (b) macrosegregation of Cu and Mg in a 200-mm round billet of a grain refined 2024 (Al-Cu-Mg) alloy cast at 120 mm/min [265].



Fig. 19. Cold crack in a 7xxx DC ingot.



(a) (b) (c)

Fig. 20. Various type of cold cracks a) and b) trouser cracks c) J-crack [192].

account for filling time, air gap formation between the billet and the bottom block as well as at the billet surface [277]. As-cast thermo-physical and thermo-mechanical properties are generated from the materials database JMatPro® [45] and partly measured experimentally [68,282].

In ALSIM5, the metal is described as an isotropic elastic-visco-plastic material in which strains are generated by thermal

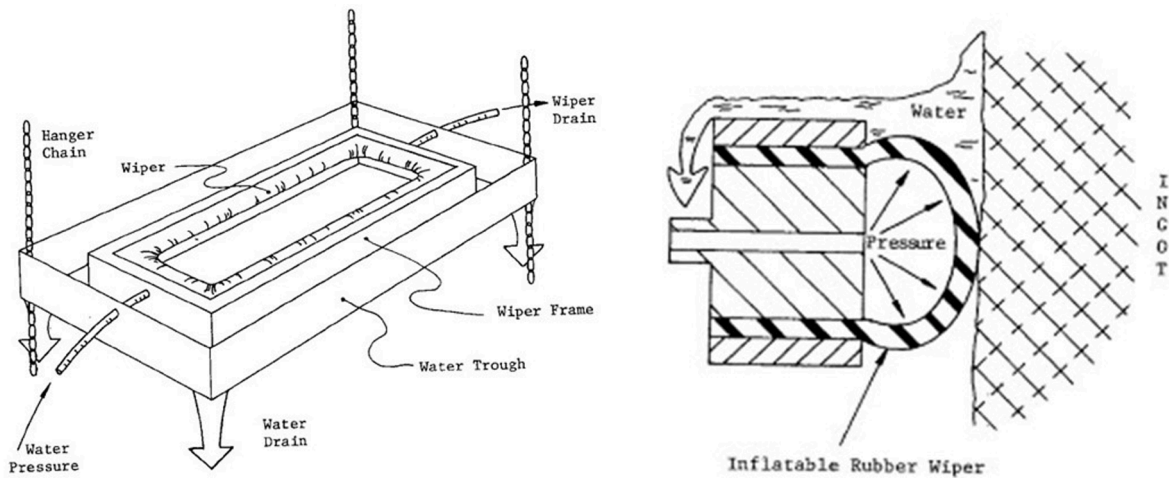


Fig. 21. Schematic view of a wiper [275].

contraction. The total visco-plastic strain is treated as one quantity [136]. Furthermore, a hardening parameter is introduced which accounts for the isotropic strain hardening of the material. In order to simulate the visco-plastic behaviour of the material, different constitutive models are used that are valid over certain temperature ranges [279]. The mathematical formulation is based on the classical small deformation theory, implying that the total strain may be divided into elastic, visco-plastic, and thermal parts. As a final result ALSIM will calculate the residual stress and distribution during DC casting.

**3.2.2.3. Cold cracking criteria.** In addition to the FEM computations a criterion is required to be able to predict cold cracking. Lalpoor et al. [283] applied fracture mechanics to determine the critical crack size for cold cracking. In this approach a penny shaped crack was chosen for the centre and mid-radius of the billet. The critical crack size (radius of the “penny”) for brittle fracture corresponding to this geometry is calculated as follows based on Griffith’s analysis [284]:

$$a_c = \frac{\pi}{4} \left( \frac{K_{Ic}}{\sigma} \right)^2 \quad (12)$$

At the surface of the billet, the surface breaking semi-circular (thumbnail) crack is chosen, for which the critical crack size is related to the  $K_{Ic}$  and nominal stress as follows [284]:

$$a_c = \frac{\pi}{(2 \times 1.13)^2} \left( \frac{K_{Ic}}{\sigma} \right)^2 \quad (13)$$

This method is more qualitative as it does not actually predict cold cracking and furthermore requires fracture toughness values at temperature for as-cast conditions. To overcome these limitations Li et al. [282] developed an alternative criterion. Under the assumption that a cold crack is the release of stored elastic strain energy from the residual stresses, the following cracking index (CCI) was proposed:

$$CCI = \frac{\sigma_1}{\sigma_0 \varphi} \quad (14)$$

$\sigma_1$  is the first principal stress,  $\sigma_0$  is a constant taken as 100 MPa, and  $\varphi$  is the ductility of the as-cast alloy.

Boender et al. [277] and Ludwig et al. [278] used the simulated maximum principal stress to assess the critical crack size that results in catastrophic failure. Alternatively, Paramatmuni et al. [204] used a stress intensity factor, that was obtained from Tada’s empirical equation [284]. Crack propagation occurs when the stress intensity factor reaches a certain value.

**3.2.2.4. Modelling results.** Drezet et al. [191] applied a thermo-mechanical model based upon the ABAQUS® software package [135] to predict successfully butt curl, but swell ingot face pull-in as indicated before in Fig. 11.

The validation of the computed stresses is largely improved by the possibility to measure the residual stresses by neutron diffraction studies. Residual strains can be measured rather deep into alloys such as aluminium and magnesium since these metals are relatively transparent to neutrons. Drezet et al [285] measured as-cast residual stresses in AA6063 with neutron diffraction techniques. By comparing the measured data with the computed results from the thermo-mechanical FE model it was found that the elimination of strain hardening has a much larger influence on the residual stress predictions as compared to the elimination of the strain rate effects. Therefore it can be concluded that the mechanical properties at low temperatures have a much larger influence on the residual stresses than those at high temperatures. Drezet et al. [286] extended this approach for an AA7050 alloy. The thermo-mechanical FE model again was able to reproduce the measured stresses and was also able to optimise the position of the wiper. The effect of a wiper on the

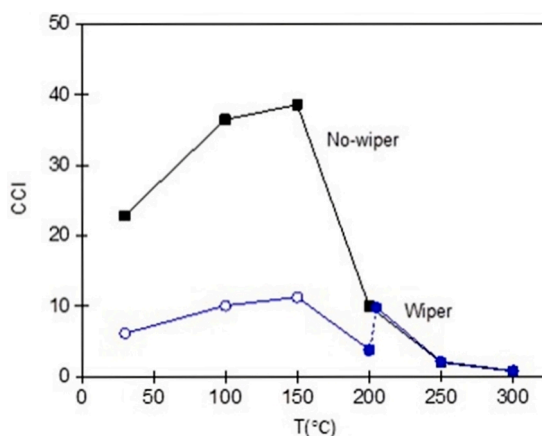


Fig. 22. Effect of a wiper on the CCI of AA7050 [282].

cold crack tendency is given in Fig. 22. Similar tendencies were reported by Boender et al. [277] and Drezet and Pirling [286].

With regard to cold cracking, Li et al. [282] calculated that AA7050 and AA7085 have the highest cracking tendencies at 150°C and 100°C respectively. They also concluded that cold cracking tendencies differ from hot cracking susceptibilities.

Calculations by Lalpoor et al. [287] revealed that the centre and the water impingement zone are the most vulnerable locations of the billet to cracking. Furthermore, with higher casting speeds or larger billet diameters the susceptible areas to cold cracking become larger in the centre. Increased temperature gradients raise the stress level in the centre, which causes a higher cracking probability.

The cold cracking criterion was validated quantitatively for an AA7050 alloy [288]. Computer simulations were followed by experimental DC-casting trials to check the critical crack sizes calculated by ALSIM5. Computer simulations were in good agreement with the experimental observations. Microstructural investigations on non-cracked billets showed that the shrinkage cavities are potential nucleation sites for cold cracking. Other defects such as hot cracks or inclusions may also reach a critical size and trigger cracking. Subroto [289] studied the connection between hot tearing and cold cracking for AA7050. For an effective cold crack criterion the dimension of a hot tear needs to be calculated. So far this is not straightforward.

### 3.3. Defects specific to shape casting

#### 3.3.1. Macro-shrinkage, sink and draw

Shape castings do not generally do not solidify all at once but progressively as described by Chvorinov [119]. Any solidification shrinkage that occurs is therefore not uniform. The definition of macro-shrinkage in this paper is the shrinkage which occurs in the top surface of the casting relative to the direction of gravity which is not fed properly during its solidification. Macro-shrinkage has been relatively easily modelled for more than the last 30 years and predictable since the 1940s. It is most often found at the tops of feeders and will be designed in to enable it to be removed at the fettling stage. Issues arise if the design is not good and the shrinkage pipe penetrates the surface of the component leaving a surface defect when the feeder is removed. Modelling the extent of the pipe therefore become extremely important to obviate any requirement for post-casting weld repairs.

If castings are not fed properly, it is also possible to create surface sinks as the liquid metal contracts in the centre of the casting. If the solid skin of the casting is thin, the internal stresses can be enough to pull in the surface, especially on larger surface areas. Sinks, which may intuitively assumed to be on the top surface of a casing can in fact occur on any large flat surface associated with a slow cooling region. Draws are shrinkage which occurs at corners as a result of the geometry causing a hot spot.

Bounds et al. [290] used Physica + software to demonstrate these defects could be modelled and were dependant largely on the freezing range of the alloy cast. Esser et al. [291] describe a continuous multiscale model that will predict the combination of gravity and fluid flow driven macro shrinkage, sinks and pipes as well as capillary controlled internal shrinkage porosity based on pore nucleation and growth. Although this was validated on a steel alloy there is no reason to believe it would not work in aluminium alloys

#### 3.3.2. Mould erosion defects and exogenous inclusions

Mould erosion defects and exogenous inclusions arise mainly when there is turbulence within the running system when using sand moulds. To the authors' knowledge there have been no models describing the physics of the process of sand erosion. Erosion of the mould occurs if the combination of the turbulence and excess heating of the mould cause a breakdown of the sand binder to the extent that that sand grains can be entrained into the liquid metal. This has been interpreted from the results of modelling the filling and the temperature of the mould and developing an experimental criterion function to indicate a probability of occurrence. This has been demonstrated for an Al-Si alloy by Sultan et al. [292] using Click-to-Cast<sup>6</sup> software.

<sup>6</sup> <https://solidthinking.com/product/inspire-cast/>.

### 3.3.3. Entrained bubbles and oxide films

The appearance of entrained bubbles and oxide films during shape casting has been well reported in the literature from the 1980s onwards [293,203,294–300] and is a result of surface turbulence developed in the liquid metal as it moves through the running system into the casting cavity. According to Runyoro et al. [301] entrainment occurs when the velocity of the liquid metal is above the critical velocity,  $v_{crit}$ , which is defined as:

$$v_{crit} = 3.52 \sqrt[4]{\frac{\gamma}{\rho}} \quad (15)$$

where  $\gamma$  is the surface tension and  $\rho$  is the density of the liquid metal. The critical velocity for surface turbulence for most engineering alloys falls between 0.4 and 0.6  $\text{ms}^{-1}$ .

Entrained bubbles have been seen in a number of cases but are especially prevalent in high pressure die casting (Fig. 23).

In order to entrain a bubble or an oxide film the surface has to be travelling at a velocity above the critical value and then fold over. There have been attempts to define when such entrainment events happen thus giving modellers the tools to embed into the standards fluid flow algorithms. Initially this was attempted in 2D for example Oxide Film Entrainment Tracking (OFET, 2-D). [302] 3D models were quickly developed as computational power increased. Most research have used some form of surface tracking using a FD/FV method [303–307]. Prakash et al. [308] used Smooth Particle Hydrodynamics (SPH) to show oxide build up and movement in foundry ingot production. A review by Reilly et al [309] describes the different mechanisms being investigated and divides them into two main categories. Indiscrete methods such as Cumulative Entrained Free Surface Area [310], Vorticity Model (MagmaSoft<sup>7</sup>), Cumulative Scalar Technique, [311] (used by most CFD codes and SPH), Code Specific Air Entrainment Models, Dimensionless Number Criteria using Weber number or Froude number [312] which have been used by Cuesta [313] and Isawa [314] and which Hsu further developed by adding an additional term to the Froude number [315]. Discrete modelling is posed as highly challenging but with the advantages that final defect locations could be identified. Most models use particles to represent oxide films but there has been little validation of these methods. Positron Emission Particle Tracking (PEPT) has been used sparingly as the experiments are complex to perform. [316]. Oxide films vary in size, shape and density and these facts make them difficult to model. Particle modelling methods [317] usually allow the modelling of spheres which can be varied in size or density and this is not enough to accurately represent oxide films.

To accurately represent entrapped bubbles it is necessary to use a multiphase model to simulate their entrainment, advection and coalescence [318]. However, the computational overhead is massive compared with single phase flow models in general this has not been a direction in which researcher have focussed their time. Kimatsuka and Kuroki [319] developed a method that looked at back pressure in the casting cavity and permeability of sand moulds and compared with real time x-ray. Their assumptions were that there was no gas flow in the cavity, the gas was ideal, there was no change of temperature, pressure or density for the gas and that the flow through the sand mould was controlled by Darcy flow. Using these assumptions they were able to realistically model the entrapment of gas in the turbulent filling an engine block casting. Majidi and Beckerman [320] have developed a model to predict the location and rate of air entrainment as part of a standard mould filling simulation. The local air entrainment rate is calculated as a function of the turbulent kinetic energy and the magnitude of the normal velocity gradient of the liquid metal at the liquid–air interface.

A number of software packages now include air entrainment as standard switches in their codes [321,322]. Such models have been used to assess the impact of running systems designed on the final quality of castings produced [323]. However, Reilly et al. [309]

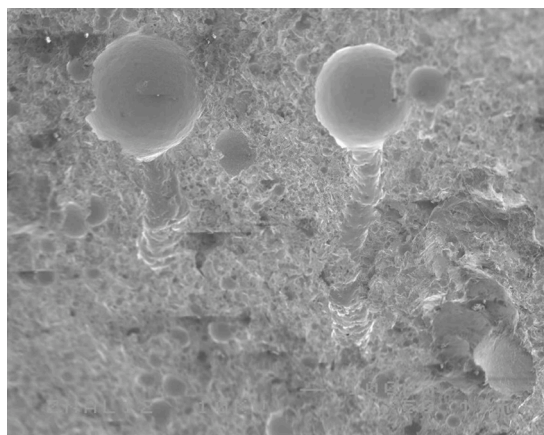


Fig. 23. SEM picture of bubbles and their trails in a die cast alloy – the largest bubble is about 0.5 mm diameter (Mehdi Divandari from [117]).

<sup>7</sup> MAGMA GmbH.



conclude that “development of quantitative defect modelling techniques is difficult and complex, but also of great industrial significance, and therefore further research is urgently required” and it would appear that this statement still largely holds true.

#### 4. Remaining challenges

Over the last 4 decades, remarkable progress has been made in the modelling of casting processes. The development of casting models is well reflected in the proceedings of the 15 Modelling of Casting, Welding and Advanced Solidification Processes (MCWASP) conferences that have been held since 1980 [15].

Computer simulations have enabled a better understanding of the physical phenomena involved during solidification. Modelling gives the opportunity to uncouple the physical processes. Furthermore, quantities that are difficult or impossible to measure experimentally can be calculated using computer simulations for example flow patterns and recalescence. However, when it comes to accurately predicting casting performance and in particular, the occurrence of defects like cracks, segregation, porosity and those where fluid flow plays a large role there is certainly some way to go.

To come to fully predictive casting models some challenges remain:

- Coupling process physics

Casting is a highly coupled phenomenon at macro and micro level. Sophisticated software is required to couple these processes and at the same time keep computing times realistic. Furthermore, most casting models are deterministic, where the real process is stochastic, and this is difficult to account for. The assumptions of symmetry to reduce computing times should be carefully considered as in most cases such symmetry mostly is not there in practise.

- Good process data for validation and process control/reproducibility

Validation and verification of casting models is essential to make them predictable. This requires good experimental process data. A major problem remaining is that the quantification of metals flows during shape and in particular DC casting is almost non-existent.

- Thermo-physical data & boundary conditions

Among the adequate description of the process physics the inclusion of accurate boundary conditions and thermo-physical data is paramount. In particular material data for metals and often mould materials throughout the casting process conditions is not readily available. An international network might be required to set up dedicated experimental program to measure and to share the data.

- Chemistry and process physics models to enable prediction of the defect formation

To arrive at a fully predictive model for defect formation a comprehensive understanding of the defect physics is required. Controlled and dedicated experiments need to be further developed to improve our current understanding.

- Evolution of the microstructure at high solid fraction is a major parameter for the prediction of defects such as porosity and hot tearing. Modelling of microstructure formation based on cellular automata models or phase-field methods, correlated with in situ observations, is necessary
- Integration of molecular dynamics, the phase-field method, cellular-automata and micro–macro modelling techniques will lead to more realistic predictions of casting processes. Three-dimensional transient modelling and incorporation of fluid flow in these models is essential.
- Faster computational algorithms and improved physical models for the calculation of multicomponent phase equilibria and improved thermodynamic data banks are fundamental for any successful simulation
- Integrated Computational Materials Engineering (ICME) framework can be used as a tool to combine computations, design and processing at the component level.

#### Declaration of Competing Interest

The authors declare that they have no known competing financial interests or personal relationships that could have appeared to influence the work reported in this paper.

**Data Statement:** Data sharing is not applicable to this article as no new data were created or analysed in this study.

#### Acknowledgements

The authors would like to acknowledge the inputs from their combined many MSc and PhD researchers, post-docs and academic colleagues with whom they have worked over the last 40 years and without whom this review would not be possible.

## Historical note

The authors first met 40 years ago at the 4<sup>th</sup> International Conference on Rapid Quenching in 1981 in Sendai, Japan where indeed they both listened to a lecture by Brian Cantor.

## References

- [1] Grealy GP, Davis JL, Jensen EK, Tondel PA, Moritz J. Advances for DC Ingot Casting: Part 1 - Introduction and Metal Distribution. In Light Metals, New Orleans; 2001.
- [2] Benedyk JC. AK's Greenfield Casthouse Produces Jumbo Billet and Slab to Supply Aerospace Al Globally. *Light Metal Age* 2017;30.
- [3] Beeley P. *Foundry Technology*. 2nd ed. Oxford: Butterworth-Heinemann; 2001.
- [4] Roth W. Verfahren zum giesen von metallblocken mit ausnahme solcher aus leichtmetallen. Germany Patent 974203, 8 9; 1938.
- [5] Ennor WT. Method of Casting. U.S.A. Patent 2301027, 3 11 1942.
- [6] Eskin DG. *Physical Metallurgy of Direct-Chill Casting of Aluminium Alloys*. Baton Raton: CRC Press; 2008.
- [7] Granfield JF, Eskin DG, Bainbridge IF. Direct-Chill Casting of Light Alloys: Science and Technology. Hoboken, New Jersey, U.S.A.: John Wiley & Sons; 2013.
- [8] C. C. Lyu, M. Papanikolaou and M. R. Jolly, Numerical Process Modelling and Simulation of Campbell Running Systems designs, in Shape Casting: 7th International Symposium Celebrating Prof. John Campbell's 80th Birthday, San Antonio, 2019.
- [9] Beckermann C, Wang CY. Incorporating interfacial phenomena in solidification models. *J Metals* 1994;46(1):42-7.
- [10] Voller VR. The evolution of solidification models. In *Fluid Flow Phenomena in Metals Processing*, Warrendale; 1999.
- [11] Wang QQ, Krane MJM, Lee PD. Simulation of aluminum shape casting processing. In *Simulation of aluminum shape casting processing*, Warrendale, PA; 2006.
- [12] Flood SC, Katgerman L, Langille AH, Rogers S, Read CM. Modelling of fluid flow and stress phenomena during DC casting of aluminium alloys. In *Light Metals*, Warrendale; 1989.
- [13] Dantzig JA, Rappaz M. Solidification. Boca Raton, FL.33487, USA: Taylor and Francis Group, LLC; 2009.
- [14] Rappaz M. Modeling of microstructure formation in solidification processes. *Int Mat Review* 1989;34:93-123.
- [15] Rappaz M. "Does MCWASP still follow Moore's law? Forty years of advances in microstructure modeling. In *Modelling of Casting, Welding and Advanced Solidification Processes XV*, Bristol, UK; 2020.
- [16] In *Modeling of Casting and Welding Processes*, Warrendale, PA; 1981.
- [17] Dantzig JA, Berry JT. *Modeling of Casting and Welding Processes II*. PA: Warrendale; 1983.
- [18] Kou S, Mehrabian R. *Modeling and Control of Casting and Welding Processes*. PA, USA: Warrendale; 1986.
- [19] Giamei AF, Abbaschian GJ. *Modeling and Control of Casting and Welding Processes IV*. PA USA: Warrendale; 1988.
- [20] Rappaz M, Özgü MR, Mahin KW. *Modeling of Casting, Welding and Advanced Solidification Processes V*. PA USA: Warrendale; 1990.
- [21] Piwonka TS, Voller V, Katgerman L. *Modeling of Casting, Welding and Advanced Solidification Processes VI*. PA, USA: Warrendale; 1993.
- [22] Cross M, Campbell J. *Modeling of Casting, Welding and Advanced Solidification Processes VII*. PA USA: Warrendale; 1995.
- [23] Thomas BG, Beckermann C. *Modeling of Casting, Welding and Advanced Solidification Processes VIII*. PA USA: Warrendale; 1998.
- [24] Sahn PR, Hansen PN, Conley JG. *Modeling of Casting, Welding and Advanced Solidification Processes IX*. PA, USA: Warrendale; 2000.
- [25] Stefanescu DM, Warren JA, Jolly MR, Krane MJM. *Modeling of Casting, Welding and Advanced Solidification Processes X*. PA USA: Warrendale; 2003.
- [26] Gandin CA, Bellet, *Modeling of Casting, Welding and Advanced Solidification Processes XI*, Warrendale, PA USA.
- [27] Cockcroft SL, Majjer DM. *Modeling of Casting, Welding and Advanced Solidification Processes XII*. PA USA: Warrendale; 2009.
- [28] Ludwig A, Wu M, Kharicha A. *Modeling of Casting, Welding and Advanced Solidification Processes XIII*. UK: Bristol; 2012.
- [29] Yasuda H. *Modeling of Casting, Welding and Advanced Solidification Processes XIV*. UK: Bristol; 2015.
- [30] Olofsson J, Dahle A, Hattel J. *Modeling of Casting, Welding and Advanced Solidification Processes XV*. UK: Bristol; 2020.
- [31] *Modelling of Casting, Welding And Solidification Processes (MCWASP) I-XIV*. Warrendale: TMS; 1980-2015.
- [32] Flood SC, Katgerman L, Voller VR. The calculation of macrosegregation and heat and fluid flows in DC casting of aluminium alloys. In *MCWASP V*, Warrendale; 1991.
- [33] Raffourt C, Fautrelle Y, Meyer JL, Hannart B. Liquid metal distribution in a slab DC casting: Experiments and modeling approach. *MCWASP V*; 1991, pp. 691-98.
- [34] Devadas C, Grandfield JF. Experiences with modelling DC casting of aluminium. In *Light Metals*, Warrendale; 1991.
- [35] Grun GU, Schneider W. Influence of fluid flow field and pouring temperature on thermal gradients in the mushy zone during level pour casting of billets. In *Light Metals*, Warrendale; 1997.
- [36] Mo A, Rusten T, Thevik HJ. Modeling of surface segregation development during DC casting of rolling slab ingots. In *Light Metals*, Warrendale; 1997.
- [37] Reddy AV, Beckermann C. Modeling of macrosegregation due to thermosolutal convection and contraction-driven flow in direct chill continuous casting of an Al-Cu round ingot. *Metall Mater Trans* 1997;28B:479-89.
- [38] Jolly MR. Examples of Practical Solutions for Aluminium Castings using Quiescent Running Systems and Computer Modelling. In 1st International Conference on Gating, Filling and Feeding of Aluminum Castings, Nashville; 1999.
- [39] Smith A, Jolly MR. Redesign of an industry test for hot tearing of high performance aluminium casting alloys using casting simulation software. In *Proceedings of 2nd International Symposium on Shape Casting*, Orlando, FL, USA; 2007.
- [40] Harlow F, Welch J. Numerical calculation of time-dependent viscous incompressible flow of fluid with free surface. *Phys Fluids* 1965;8:2182-9.
- [41] Nichols BD, Hirt CW, Hotchkiss RS. SOLA-VOF: A solution for transient fluid flow with multiple free boundaries. Los Alamos, NM, USA: Los Alamos Scientific Laboratory; 1980.
- [42] Rappaz M, Bellet M, Deville M. *Numerical Modelling in Materials Science and Engineering*. Heidelberg: Springer-Verlag; 2003.
- [43] Dantzig J, Tucker III C. *Modeling in Materials Processing*, Cambridge. UK: Cambridge University Press; 2001.
- [44] Yu K-O. *Modeling for Casting and Solidification Processing*, New York. USA: Marcel Dekker Inc.; 2002.
- [45] JMatPro®, Sente Software Ltd; 2011. [Online]. Available: <https://www.sentesoftware.co.uk/>.
- [46] Thermo-Calc, [Online]. Available: <http://www.thermocalc.com>.
- [47] Jones CA, Jolly MR, Jarfors AEW, Irwin M, Svenningsson R, Steggo J. A verification of thermophysical properties of a porous ceramic investment casting mould using commercial computational fluid dynamics software. *Modelling of Casting, Welding and Advanced Solidification Processes*, Bristol, UK. 2020.
- [48] Jones S, Jolly MR, Lewis K. Development of techniques for predicting ceramic shell properties for investment casting. *British Ceramics Transactions* 2002;101(3):106-13.
- [49] M. Salmonds, Interviewee, [Interview]; 2001.
- [50] Williams K, Snider D, Walker M, Palczewski SA. Process modeling: Sand core blowing. *Transactions of the American Foundry Society*, Schaumburg, Illinois, United States. 2002.
- [51] Thorborg J, Kumar S, Wagner I, Sturm JC. The virtual core - modelling and optimization of core manufacturing and application. *Modelling of Casting, Welding and Advanced Solidification Processes*, Bristol, UK. 2020.
- [52] Moriceaux J. Thermal stresses in continuous DC casting of Al alloys, discussion of hot tearing mechanisms. In *Light Metals*, New York, NY; 1975.
- [53] Fjaer HG, Mo A. ALSPEN-, A mathematical model of thermal stresses in direct chill casting of aluminium billets. *Metall TransB* 1990;21:1049-61.
- [54] van Haften WM, Magnin B, Kool WH, Katgerman L. Constitutive behavior of as-cast AA1050, AA3104, and AA5182. *Metall Mater Trans A* 2002;33A:1971-80.
- [55] Ludwig P. *Elemente der Technologischen Mechanik*. Berlin: Springer-Verlag OHG; 1909.

- [56] Magnin B, Maenner L, Katgerman L, Engler S. Ductility and Rheology of an Al-4.5% Cu Alloy from Room Temperature to Coherency Temperature. *Mat Sci Forum* 1996;217–222:1209–14.
- [57] Soni A, Alankar A. Analysis of constitutive behavior of as-cast AA3104, AA5182 and AA6011 during direct chill casting using physically based models. *ASME J Eng Mater Technol* 2019;141.
- [58] Alankar A, Wells MA. Constitutive behavior of as-cast aluminum alloys AA3104, AA5182 and AA6111 at below solidus temperatures. *Mater Sci Eng A* 2010; 527:7812–20.
- [59] Kocks UF. Laws for Work-Hardening and Low-Temperature Creep. *ASME J Eng Mater Technol* 1976;98:76–85.
- [60] Choudhary BK, Christopher J. Tensile Work Hardening Behavior of Thin-Section Plate and Thick-Section Tubeplate Forging of 9Cr-1Mo Steel in the Framework of One-Internal-Variable Kocks-Mecking Approach. *Metall Mater Trans A* 2013;44:4968–78.
- [61] Braccini M, Martin CL, Suéry M, Bréchet Y. Relation between mushy zone rheology and hot tearing phenomena in Al-Cu alloys. In *MCWASP IX, Aachen*; 2000.
- [62] Suyitno WH, Kool, Katgerman L. Finite element method simulation of mushy zone behavior during direct-chill casting of an Al-4.5 pct Cu alloy. *Metall Mater Trans A* 2004;35:2917–26.
- [63] M'Hamdi M, Benum S, Mortensen D, Fjaer H, Drezet J-M. The importance of viscoplastic strain rate in the formation of center cracks during the start-up phase of direct-chill cast aluminum extrusion ingots. *Metall Mater Trans* 2003;A:1941–52.
- [64] Drezet J, Eggeler G. High apparent creep activation energies in mushy zone microstructures. *Scripta Metal Mater* 1994;31:757–62.
- [65] van Haafden WM, Kool WH, Katgerman L. Tensile behaviour of semi-solid AA3104 and AA5182. *Mater Sci Eng A* 2002;336:1–6.
- [66] Wray PJ. The geometry of two-phase aggregates in which the shape of the second phase is determined by its dihedral angle. *Acta Metall* 1976;24:125–35.
- [67] Fabreque D, Deschamps A, Suéry M, Poole WJ. Rheological behavior of Al-Mg-Si-Cu alloys in the mushy state obtained by partial remelting and partial solidification at high cooling rate. *Metall Mater Trans A* 2006;37:1459–67.
- [68] Subroto T, Miroux A, Eskin DG, Katgerman L. Tensile mechanical properties, constitutive parameters and fracture characteristics of an as-cast AA7050 alloy in the near-solidus temperature regime. *Mater Sci Eng A* 2017;679:28–35.
- [69] Subroto T, Miroux A, Eskin DG, Katgerman L. Constitutive behaviour of an as-cast AA7050 alloy. *Mater Sci Eng* 2011;27:012074.
- [70] Subroto T, Eskin D, Miroux A. M. M'Hamdi and I. Katgerman, Semi-solid constitutive parameters and failure behaviour of a cast AA7050 alloy. *Metall Mater Trans A* 2021;52A:871–88.
- [71] Takai R, Matsushita A, Yanagida S, Nakamura K, Yoshida M. Development of an elasto-viscoplastic constitutive equation for an Al-Mg alloy undergoing a tensile test during partial solidification. *Mater Trans* 2015;56(8):1233–41.
- [72] Phillion AB, Cockcroft SL, Lee PD. A three-phase simulation of the effect of microstructural features on semi-solid tensile deformation. *Acta Mater* 2008;56: 4328–38.
- [73] Phillion AB, Cockcroft SL, Lee PD. A new methodology for measurement of semi-solid constitutive behavior and its application to examination of as-cast porosity and hot tearing in aluminum alloys. *Mat Sci Eng A* 2008;491:237–47.
- [74] Phillion AB, Cockcroft SL, Lee PD. Predicting the constitutive behavior of semi-solids via a direct finite element simulation: application to AA5182. *Modelling Simul Mater Sci Eng* 2009;17:055011.
- [75] Jamaly N, Phillion AB, Drezet J-M. Stress-Strain Predictions of Semisolid Al-Mg-Mn Alloys During Direct Chill Casting: Effects of Microstructure and Process Variables. *Metall Mater Trans B* 2013;44:1287–95.
- [76] Phillion AB, Hamilton RW, Fuloria D, Leung ACL, Rockett P, Connolley T, et al. In situ X-ray observation of semi-solid deformation and failure in Al-Cu alloys. *Acta Mater* 2011;59:1436–44.
- [77] Spittle JA, Cushway AA. Influences of superheat and grain structure on hot-tearing susceptibilities of Al-Cu alloy castings. *Metals Technol* 1983;10:6–13.
- [78] Ohm L, Engler S. Festigkeitseigenschaften erstarrender Randschalen aus Al-Legierungen. *Giessereiforschung* 1990;42(3):131–62.
- [79] Instone S, StJohn D, Grandfield JF. New apparatus for characterising tensile strength development and hot cracking in the mushy zone. *Int J Cast Metals Res* 2000;12:441.
- [80] Eskin DG, Suyitno JF. Mooney and L. Katgerman, Contraction of Aluminum Alloys during and after Solidification. *Metall Mater Trans A* 2004;35:1325–35.
- [81] Zhang L, Eskin DG, Lalpou M, Katgerman L. Factors affecting thermal contraction behavior of an AA7050 alloy. *Mater Sci Eng A* 2010;527:3264–79.
- [82] Li Y, Zhang ZR, Zhao ZY, Li HXKL. Effect of main elements (Zn, Mg, and Cu) on hot tearing susceptibility during direct-chill casting of 7xxx aluminum alloys. *Metall Mater Trans A* 2019;50A:3603–16.
- [83] Kayikci E, Griffiths WD. The influence of surface roughness on interfacial heat transfer during casting solidification. In *Proceedings of the Annual Conference of the Institute of British Foundrymen (Castcon '98)*, Alvechurch, Birmingham, UK; 1998.
- [84] Hallam C. Interfacial heat transfer between solidifying aluminium alloys and coated die steels. Manchester: University of Manchester Institute of Science and Technology; 2001.
- [85] Drezet JM, Rappaz M, Grün GU, Gremaud M. Determination of thermophysical properties and boundary conditions of direct chill-cast aluminum alloys using inverse methods. *Metall Mater Trans A* 2000;31 A:1627–34.
- [86] Bilal MU, Hort N. Predicting the interfacial heat transfer coefficient of cast Mg-Al alloys using Beck's inverse analysis. *Modelling of Casting, Welding and Advanced Solidification Processes*, Bristol, UK. 2020.
- [87] Zapulla MLS, Thomas BG. Simulation of longitudinal surface defect in steel continuous casting, in *Modelling of Casting*. Bristol, UK: Welding and Advanced Solidification Processes; 2020.
- [88] Wen SW, Hastings N, Jolly MRMR. *Modelling of Filling in Crankshaft Castings*. Birmingham, UK: Casting Centre; 1998.
- [89] Jolly MR, Lo HSH, Turan M, Campbell J, Yang X. Development of Practical Quiescent Running Systems without Foam Filters for use in Aluminium Castings using Computer Modelling. *Modelling of Casting, Welding and Advanced Solidification Processes*, Aachen. 2000.
- [90] Nwaogu UC, Tiedje NS. Foundry Coating Technology: A Review. *Mater Sci Appl* 2011;2:1143–60.
- [91] Pehlke RD, Berry JT. Investigation of Heat Transfer at the Mold/Metal Interface in Permanent Mold Casting of Light Alloys. *USDOE Office of Industrial Technologies (OIT) - (EE-20)*; 2005.
- [92] Rafique MMA, Iqbal J. Modeling and simulation of heat transfer phenomena during investment casting. *Int J Heat Mass Transf* 2009;52(7–8):2132–9.
- [93] Angladaa E, Meléndez A, Maestro L, Domínguez I. Adjustment of Numerical Simulation Model to the Investment. *Procedia Eng* 2013;63:75–83.
- [94] Mollibog T, Littleton HE. Experimental simulation of pattern degradation in lost foam. *Transactions of the American Foundry Society*, Schaumburg, Illinois, United States. 2001.
- [95] Mirbagheri SMH, Serajzadeh S, Varahram N, Davami P. Modelling of foam degradation in lost foam casting process. *Mater Des* 2006;27:115–24.
- [96] Kahn S, Ravindran C, Naylor D. Effect of casting section thickness and coating thickness on the interfacial heat transfer coefficient in lost foam casting. *Transactions of the American Foundry Society*, Schaumburg, Illinois, United States. 2001.
- [97] Gunasegaram DR, Finnin BR, Polivka FB. Melt flow velocity in high pressure die casting: its effect on microstructure and mechanical properties in an Al-Si alloy. *Mater Sci Technol* 2007;23(7):847–56.
- [98] Cleary PW, Ha J, Prakash M, Nguyen T. 3D SPH flow predictions and validation for high pressure die casting of automotive components. *Appl Math Model* 2006;30(11):1406–27.
- [99] Magmasoft, *Die Casting: Optimized Quality, Robust Tooling and Cost Effective Processes*, Aachen, D.
- [100] Anglada E. A. Meléndez I, I. Vicario, E. Arratibel and G. Cangas, Simplified Models for High Pressure Die Casting Simulation. *Procedia Eng* 2015;132:974–81.
- [101] Lee PD. Defects in aluminium shape casting. In *Solidification and Casting*. London & Philadelphia, IOP; 2003, p. 121–41 [Chapter 9].
- [102] Khalajzadeh V, Goetsch DD, Beckermann C. Real-time X-ray Radiography and Computational Modeling of Shrinkage Porosity Formation in Aluminum Alloy Castings. *Metall Mater Trans A* 2018;50(4):1–15.
- [103] Khalajzadeh V, Beckermann C. Simulation of Shrinkage Porosity Formation During Alloy Solidification. *Metall Mater Trans A* 2020;51(4).
- [104] Zhu JD, Cockcroft SL, Majjer DM. Modeling of microporosity formation in A356 aluminum alloy casting. *Metall Mater Trans A* 2006;37:1075–85.
- [105] Zhu JD, Cockcroft S, Majjer DM, Ding R. Simulation of microporosity in A356 aluminium alloy castings. *Int J Cast Met Res* 2005;18(4):229–35.

- [106] Iqbal H, Sheikh AK, Al-Yousef AH, Younas M. Mold Design Optimization for Sand Casting of Complex Geometries Using Advance Simulation Tools. *Mater Manuf Processes* 2012;27(7):775–85.
- [107] Jolly MR. Casting simulation: How well do reality and virtual casting match? State of the art review. *Int Journal of Cast Metals Research* 2002;14:303–13.
- [108] Khan MAA. A comparative study of simulation software for modelling metal casting processes. *Int J Simul Model* 2018;17(2):197–209.
- [109] Ziolkowski JE. Modeling of an aerospace sand casting process. Worcester, MA, USA: Worcester Polytechnic Institute; 2002.
- [110] Gebelin J-C, Jolly MR. Numerical modeling of metal flow through filters. *Modelling of Castings, Welding and Advanced Solidification Processes*, San Destin. 2003.
- [111] Bolduc S, Kiss L. Sensitivity study of the influence of the water boiling parameters on aluminium semi-continuous DC casting. *Int J Therm Sci* 2020;151:106276.
- [112] Fu J, Coleman J, Poole G, Krane M, Marconnet A. Uncertainty propagation through a simulation of industrial high pressure die casting. *J Heat Transfer-Trans ASME* 2019;141(11):112101.
- [113] Zindani D, Maity S, Blowmik S. A concurrent decision-making approach toward uncertainty, vagueness and risk appetite for sustainable manufacturing processes. *Clean Technol Environ Policy* 2020.
- [114] Griffiths WD, Cox M. Quality indices for modelling of mould filling. Birmingham: University of Birmingham; 2001.
- [115] Pagone E, Papanikolaou M, Salonitis K, Jolly M. Multi-criteria decision-making for the life cycle of sustainable high pressure die casting products. *Int J Sustain Manuf* 2020;4(2–4):101–20.
- [116] Papanikolaou M, Pagone E, Salonitis K, Jolly M. Sustainability-Based Evaluation of Casting Gating Systems: a Multi-Criteria Decision-Making Approach. *Procedia Manuf* 2020;43:704–11.
- [117] Jolly M. Castings. In Karihaloo BL, Milen I, RRO, editors, *Comprehensive structural integrity*, vol. 1. Elsevier; 2003.
- [118] Steinbach I, Schmitz GJ. Direct numerical simulation of solidification structure using the phase field method. *Proceedings of 8th Conference on Modeling of Casting, Welding and Advanced Solidification Processes (McWASP VIII)*, Warrendale, PA. 1998.
- [119] Chvorinov N. Theory of solidification of castings. *Giesserei* 1940;27:201–8.
- [120] Wlodawer R. *Directional Solidification of Steel Castings*. Oxford.: Pergamon; 1966.
- [121] Niyama E, Uchida T, Morikawa M, Saito S. A method of shrinkage prediction and its application to steel casting practice. *Int J Cast Metals Res* 1982;7:52–63.
- [122] Flemings MC. *Solidification Processing*. New York, NY, USA: McGraw Hill; 1974.
- [123] Zienkiewicz OC, Taylor RL, Zhu JZ. *The Finite Element Method: Its basis and fundamentals*. 6th ed. Oxford: Elsevier; 2005.
- [124] Jolly MR, Wen SW, Campbell J. An overview of numerical modelling of casting processes. In *Proceedings of Conference on Modelling and Simulation*, Beijing, China, June 11–13; 1996.
- [125] Magmasoft GmbH, [Online]. Available: <https://www.magmaflow.com/en/>. [Accessed July 2020].
- [126] ESI-ProCast, [Online]. Available: <https://www.esi-group.com/products/casting> [Accessed July 2020].
- [127] NovaFlow&Solid, [Online]. Available: <https://www.novacast.se/product/novaflowsolid/> [Accessed July 2020].
- [128] [Online]. Available: <https://www.anycastsoftware.com:32102/eng/> [Accessed July 2020].
- [129] Finite Solutions, [Online]. Available: <https://finite.solutions/finite-solutions-metal-casting-simulation-software/> [Accessed July 2020].
- [130] Flow-3D, [Online]. Available: <https://www.flow3d.com/>.
- [131] ANSYS-CFX, [Online]. Available: <https://www.ansys.com/products/fluids/ansys-cfx>.
- [132] ANSYS-Fluent, [Online]. Available: <https://www.ansys.com/products/fluids/ansys-fluent>.
- [133] ANSYS, ANSYS Inc., [Online]. Available: <https://www.ansys.com/>.
- [134] MARC, MSC Company, [Online]. Available: <https://www.mscsoftware.com/product/marc>.
- [135] Dassault Systems Inc, [Online]. Available: <https://www.3ds.com/products-services/simulia/?woc=%7B%22brand%22%3A%5B%22brand%2Fsimulia%22%5D%7D>.
- [136] Mortensen D. A mathematical model of the heat and fluid flows in direct-chill casting of aluminum sheet ingots and billets. *Metall Trans* 1999;30B:119–33.
- [137] Mortensen D, Fjaer HG, Lindholm D, Rudshaug M, Sorheim EA. The development of ALSIM- a modelling tool for direct chill casting, twin roll casting, wheel and belt casting and chain conveyor casting. *Mater Sci Forum* 2011;693:187–95.
- [138] Li BQ, Anyalebechi PN. A micro/macro model for fluid flow evolution and microstructure formation in solidification processes. *Int J Heat Mass Transfer* 1995;38:2367–81.
- [139] Henriksen BR, Jensen EK, Mortensen D. The modelling of transient heat and fluid flow in the start-up phase of the DC casting process. In *MCWASP VIII*, Warrendale; 1998.
- [140] Gandin C-A, Jalanti TT, Rappaz M. Modeling of dendrite grain structures. *Proceedings of 8th Conference on Modeling of Casting, Welding and Advanced Solidification Processes*, Warrendale, PA. 1998.
- [141] Li H, Mulay SS. *Meshless Methods and Their Numerical Properties*. Baton Raton: CRC Press; 2013.
- [142] Liu GR. *Mesh Free Methods: Moving beyond the Finite Element Method*. Boca Raton: CRC Press; 2009.
- [143] Kosec G, Sarler G. Simulation of macrosegregation with mesosegregates in binary metallic casts by a meshless method. *Eng Anal Boundary Elem* 2014;45:36–44.
- [144] Cleary PW, Prakash M, Ha J, Stokes N, Scott C. Smooth particle hydrodynamics: status and future potential. *Progr Comput Fluid Dyn* 2007;7(2–4).
- [145] Asta M, Beckermann C, Karma A, Kurz W, Napolitano R, Plapp M, et al. Solidification microstructures and solid-state parallels: Recent developments, future directions. *Acta Mater* 2009;57:941–71.
- [146] Ni J, Beckermann C. A Volume-Averaged Two-Phase Model for. *Met Trans* 1991;22B:349–61.
- [147] Wang CY, Beckermann C. Equiaxed dendritic solidification with convection: Part I. Multiscale/multiphase modeling. *Metall Mater Trans* 1996;27A:2754–64.
- [148] Kurz WD, Trivedi R. Progress in modelling solidification microstructures in metals and alloys: dendrites and cells from 1700 to 2000. *Int Mater Review* 2019;64:311–54.
- [149] Kurz W, Rappaz M, Trivedi R. Progress in modelling solidification microstructures in metals and alloys. Part II: dendrites from 2001 to 2018. *Int Mat Review* 2021;66(1):30–76.
- [150] Jacot A. A cellular automaton approach for the prediction of grain size in grain refined alloys. *Modelling of Casting, Welding and Advanced Solidification Processes XV*, Bristol, UK. 2020.
- [151] Anderson MP, Srolovitz DJ, Grest GS, Sahn PS. Computer simulation of grain growth—I. Kinetics. *Acta Metall* 1984;32:783–91.
- [152] Spittle JA, Brown SGR. Computer simulation of the effects of alloy variables on the grain structures of castings. *Acta Metall* 1989;37:1803–10.
- [153] Rappaz M, Gandin C-A. Probabilistic modelling of microstructure formation in solidification processes. *Acta Metall Mater* 1993;41(2):345–60.
- [154] Karma A, Tourret D. Atomistic to Continuum Modeling of Solidification Microstructures. *Curr Opin Solid State Mater Sci* 2015;20:25–36.
- [155] Jarry P, Rappaz M. Recent advances in the metallurgy of aluminium alloys. Part I: Solidification and casting. *C RPhysique* 2018;19:672–87.
- [156] Reuther K, Rettenmayr M. Perspectives for cellular automata for the simulation of dendritic solidification – A review. *Comput Mater Sci* 2014;95:213–20.
- [157] Carozzani T, Digonnet H, Gandin C. 3D CAFE modelling of grain structures: application to primary dendritic and secondary eutectic solidification. *Modell Simul Mater Sci Eng* 2012;20(1):015010.
- [158] Jarvis DJ, Brown SGR, Spittle JA. A 2D cellular automaton-finite difference (CAFD) model of the solidification of Al–Cu–Si alloys. *Proceedings of Conference on Light Metals*. 2000.
- [159] Warren JA, Boettinger WJ. Prediction of dendritic growth and microsegregation patterns in a binary alloy using the phase-field method. *Acta Metall Mater* 1995;43:689–703.
- [160] Boettinger WJ, Warren JA, Beckermann C, Karma A. Phase Field Simulation of Solidification. *Annu Rev Mater Res* 2002;32:1630194.
- [161] Steinbach I. Phase field models in materials science. *Modell Simul Mater Sci Eng* 2009;17(7):073001.
- [162] Qin RS, Bhadesia HK. Phase field method. *Mater Sci Technol* 2010;26(7):803–11.

- [163] Provatas N, Kelder K. Phase-Field Methods in Materials Science and Engineering. Weinheim, Germany: Wiley- VCH Verlag; 2010.
- [164] Dobračeva T, Mavriča BSB. Reduction of discretisation-induced anisotropy in the phase-field modelling of dendritic growth by meshless approach. *Comput Mater Sci* 2020;172:109166.
- [165] Warren JA, George W. NIST; 2002.
- [166] Tourret D, Sturz L, Viardín A, Založnik M. Comparing mesoscopic models for dendritic growth. *Modelling of Casting, Welding and Advanced Solidification Processes XV*, Bristol, UK. 2020.
- [167] Wang Y, Li J. Phase field modeling of defects and deformation. *Acta Mater* 2010;58(4):1212–35.
- [168] Li Y, Hu S, Sun X, Stan M. A review: applications of the phase field method in predicting microstructure and property evolution of irradiated nuclear materials. *NPJ Comput Mater* 2017;16.
- [169] Wang N, Kocher G, Provatas N. A phase-field-crystal alloy model for late-stage solidification studies involving the interaction of solid, liquid and gas phases. *Philos Trans A Math Phys Eng Sci.* 2018;376(2113).
- [170] Fujinaga T, Shibuta Y. Molecular dynamics simulation of heterogeneous nucleation from concave cavity at surface of grain refiner. *Modelling of Casting, Welding and Advanced Solidification Processes*, Bristol, UK. 2020.
- [171] Papanikolaou M, Salonitis K, Jolly MR. Molecular Dynamics Simulations of the Evolution of Residual Stresses During Rapid Solidification of Aluminium. In *Light Metals 2021: 50th Anniversary Edition, On-Line*; 2021.
- [172] Richter R, DeYoung D. Control of rolling ingot surface quality. In *Aluminium Cast House Technology 2007*, Sydney; 2007.
- [173] Bergmann W. Solidification in Continuous Casting of Aluminium. *Metallurgical Transactions* 1970;1:3361–4.
- [174] Weckmann D, Niessen P. The Mechanism of Cold Shut Formation on D.C. Continuously Cast Non-Ferrous Alloy Products. *Zeitschrift für Metallkunde* 1984;75: 414–22.
- [175] Weckmann D, Niessen P. Heat-transfer conditions in hot-top mould and cold-shut formation mechanism on DC continuously cast non-ferrous alloy rods. *Metals Technol* 1984;11(1):497–503.
- [176] Buxmann K. Mechanismen der Oberflächenseigerung von Strngguss. *Metall* 1977;31(2):163–70.
- [177] Mo A. Mathematical modelling of surface segregation in aluminium DC casting caused by exudation. *Int J Heat Mass Transfer* 1993;36(18):4335–40.
- [178] Benum S, Hakonson A, Hafsas J, Siversen J. Mechanisms of surface formation during Direct Chill (DC) casting of extrusion ingots. In *Light Metals 1999*, Warrendale; 1999.
- [179] Mo A, Rusten T, Thevik H, Henriksen B, Jensen E. Modelling of surface segregation development during DC casting of rolling slab ingots. In *Light Metals 1997*, Warrendale; 1997.
- [180] Mortensen D, Henriksen B, M'Hamdi M, Fjaer H. Coupled modelling of air-gap formation and surface exudation during extrusion ingot DC casting. In *Light Metals 2008*, Warrendale; 2008.
- [181] Hsu F-Y, Yang Y-M. Confluence weld in an aluminum gravity casting. *J Mater Process Technol* 2012;212(4):825–40.
- [182] Cao L, Liao D, Sun F, Chen T. Numerical simulation of cold-lap defects during casting filling process. *Int J Adv Manuf Technol* 2018;97:2419–30.
- [183] Bhone NR. Prediction of blow holes in sand casting, Bombay; 2004.
- [184] Cross M, Bailey C, Pericleous K, Croft TN, Williams A, Slone A, et al. *Introduction to Process Modelling*. London: University of Greenwich; 2001.
- [185] Bellet M, Thomas BG. Solidification Macroprocesses (Modeling of stress, distortion and hot tearing). In: *Materials Processing Handbook*. CRC Press; 2007. p. 27.
- [186] Hofer P, Kaschnitzl E, Schumacherl P. Simulation of distortion and residual stress in high pressure die casting – modelling and experiments. In *Modeling of Casting, Welding and Advanced Solidification Processes XIII*, Schladming, Austria; 2012.
- [187] Miller RA. Prediction of Part Distortion in Die Casting: DE-FC07-97ID13577, Department of Energy; 2002.
- [188] Ahlstrom J, Larsson R. Modeling of Distortion during Casting and Machining of Aluminum Engine Blocks With Cast-in Gray Iron Liners. *Mater Perform Charact* 2012;1(1):1–19.
- [189] Hakonson A. A model to predict the steady state pull-in during DC casting of aluminium sheet ingots. In *Light Metals 1997*, Warrendale; 1997.
- [190] Fjaer H, Hakonson A. The mechanism of pull-in during DC casting of aluminium sheet ingots. In *Light Metals 1997*, Warrendale; 1997.
- [191] Drezet J-M, Rappaz M. Modeling of ingot distortions during direct chill casting of aluminum alloys. *Metall Mater Trans A* 1996;27A:3214–25.
- [192] Boender W, Burghardt A, van Klaveren EP, Rabenberg J. Numerical simulation of DC casting: Interpreting the results of a thermo-mechanical model. In *Light Metals*, Warrendale; 2004.
- [193] Droste WE, Grun GU, Schneider W, Drezet J-M. Thermo-mechanical modeling to predict shrinkage, shape and mold openings for DC-cast rolling ingots. In *Light Metals*, Warrendale; 2002.
- [194] Schneider W, Droste W. Laboratory Investigations about the Influence of Starting Conditions on Butt Curl and Swell of D.C. Cast Sheet Ingots. *Light Metals*, Warrendale. 1991.
- [195] Kolby P, M'Hamdi M, Mo A, Nielsen Ø, Mispic P. Interdendritic bridging and hot tearing modeling. *Transactions of the American Foundry Society*, Schaumburg, Illinois, United States. 2002.
- [196] Yang BJ, Smith RW, Sahoo M, Sadayappan M. How the Marangoni force is important for hot tearing tendency. *Transactions of the American Foundry Society*, Schaumburg, Illinois, United States. 2002.
- [197] Li S. *Hot Tearing in Cast Aluminum Alloys: Measures and Effects of Process Variables*. Worcester Polytechnic Institute; 2010.
- [198] Shyam A, Haynes JA, Black G, Talamantes J. *High Performance Cast Aluminum Alloys for Next Generation Passenger Vehicle Engines*. Oakridge: ORNL; 2018.
- [199] Sabau A. Modeling of casting defects in an integrated computational materials engineering approach. In *Advances in the Science and Engineering of Casting Solidification*, Warrendale; 2015.
- [200] Chen D, Wang J, Zhang C. Coupling phase-field model and CFD for hot cracking predictions of Al-Li alloys. *Comput Mater Sci* 2021;192:110361.
- [201] Quak CJ. Rheology of partially solidified aluminum alloys and composites. Delft: PhD Thesis Delft University of Technology; 1996.
- [202] Eskin DG, Katgerman L. A Quest for a New Hot Tearing Criterion. *Metall Mater Trans A* 2007;38A:1511–9.
- [203] Campbell J. *Castings*. Oxford: Butterworth-Heinemann; 2003.
- [204] Paramatmuni RK, Chang K-M, Kang BS, Liu X. Evaluation of cracking resistance in DC casting high strength aluminum ingots. *Mat Sci Eng* 2004;A:293–301.
- [205] Eskin DG, Suyitno and L. Katgerman, Mechanical properties in the semi-solid state and hot tearing of aluminium alloys. *Prog Mat Sci* 2004;49:629–711.
- [206] Suyitno. *Hot Tearing and Deformation in Direct-Chill Casting of Aluminium Alloys*. Delft: PhD Thesis; 2005.
- [207] Du Q, Jacot A. A two-dimensional microsegregation model for the description of microstructure formation during solidification in multicomponent alloys: Formulation and behaviour of the model. *Acta Mater* 2005;53:3479–93.
- [208] Granfield JF, Wang L. Application of mathematical models to optimization of cast start practice for DC cast extrusion billets. In *Light Metals*, Warrendale; 2004.
- [209] Schneider W, Jensen EK. Investigations about Starting Cracks in D.C. Casting of 6063 Type Billets. Part I Experimental Results. *Light Metals*, Warrendale. 1990.
- [210] Jensen EK, Schneider W. Investigations about Starting Cracks in D.C. Casting of 6063 Type Billets. Part II Modelling Results. *Light Metals*, Warrendale. 1990.
- [211] Martin CL, Braccini M, Suéry M. Rheological behaviour of the mushy zone at small strains. *Mater Sci Eng A* 2002;325:293–302.
- [212] Suyitno, Kool WH, Katgerman L. Integrated Approach for Prediction of Hot Tearing. *Metall Mater Trans A* 2009;40:2388–400.
- [213] Farup I, Mo A. Two-phase modelling of mushy zone parameters associated with hot tearing. *Metall Mater Trans A* 2000;31A:1461–72.
- [214] Bai QL, Liu JC, Li HX, Du Q, Katgerman L, Zhang JS, et al. A modified hot tearing criterion for direct chill casting of aluminium alloys. *Mat Sci Techn* 2016;32: 846–54.
- [215] M'Hamdi M, Mo A, Fjaer HG. TearSim: A two-phase model addressing hot tearing formation during aluminum direct chill casting. *Metall Mater Trans A* 2006; 37:3069–83.
- [216] Sistaninia M, Phillion AB, Drezet J-M, Rappaz M. A 3-D coupled hydromechanical granular model for simulating the constitutive behavior of metallic alloys during solidification. *Acta Mater* 2012;60:6793–803.
- [217] Rappaz M, Drezet J-M, Gremaud M. A new hot tearing criterion. *Metall Mater Trans A* 1999;30:449–55.

- [218] Sistaninia M, Terzi S, Phillion AB, Drezet J-M, Rappaz M. 3-D granular modeling and in situ X-ray tomographic imaging: A comparative study of hot tearing formation and semi-solid deformation in Al-Cu alloys. *Acta Mater* 2013;61:3831–41.
- [219] Sistaninia M, Drezet J-M, Phillion AB, Rappaz M. Prediction of Hot Tear Formation in Vertical DC Casting of Aluminum Billets Using a Granular Approach. *JOM* 2013;65:1131–7.
- [220] Rappaz M. Modeling and characterisation of grain structures and defects in solidification. *Curr Opin Solid State Mater Sci* 2016;20:37–45.
- [221] Taylor RP, Shenfelt J, Berry JT, Luck R. Comparison of and criticism of casting criteria functions. *Transactions of the American Foundry Society, Schaumburg, Illinois, United States*. 2002.
- [222] Zhu JD, Cockcroft SL, Maijer DM. Modeling of microporosity formation in A356 aluminum alloy casting. *Metall Mater Trans A* 2006;37:1075.
- [223] Zhang A, Guo Z, Wang Q, Xiong S. Multiphase-field modelling of hydrogen pore evolution during alloy solidification. *Modelling of Casting, Welding and Advanced Solidification Processes XV*, Bristol, UK. 2020.
- [224] Gu C, Luo AA. Three-dimensional numerical simulation of solidification microporosity and microstructure of aluminum alloys. *Modelling of Casting, Welding and Advanced Solidification Processes XV*, Bristol, UK. 2020.
- [225] Zhang A, Guo Z, Wang Q, Xiong S. Multiphase-field modelling of hydrogen pore evolution during alloy solidification. *Modelling of Casting Welding and Advanced Solidification Processes XV*, Bristol, UK. 2020.
- [226] Lee P, Atwooda R, Dashwooda R, Nagaumi H. Modeling of porosity formation in direct chill cast aluminum – magnesium alloys. *Mater Sci Eng* 2002;A328: 213–22.
- [227] M'Hamdi M, Mo A. On modelling the interplay between microporosity formation and hot tearing in aluminum direct-chill casting. *Mater Sci Eng, A* 2005; 413–414:105–8.
- [228] Voller VR. Micro–macro modeling of solidification processes and phenomena. *Proceedings of Conference on Computational Modeling of Materials, Minerals, and Metals Processing*, Seattle, WA, USA, February 2002, Warrendale, PA. 2002.
- [229] Voller VR, Porte-Agel F. Moore's law and numerical modeling. *J Comp Physics* 2001;179(2):698–703.
- [230] Thevoz P, Gaumann M, Gremaud M. The numerical simulation of continuous and investment casting. *JOMe* 2002;54(1).
- [231] Thévoz P, Desbiolles J-L, Rappaz M. Modelling of equiaxed microstructure formation in castings. *Metall Trans* 1989;20A:311–22.
- [232] Hakonsen A, Mortensen D, Benum S, Vatne H. A micro/macro model for the equiaxed grain size distribution in DC-cast aluminium ingots. In *Light Metals 1999*, Warrendale; 1999.
- [233] Bedel M, Heyvaert L, Založnik M, Combeau H, Daloz D, Lesoult G. Process-scale modelling of microstructure in direct chill casting of aluminium alloys. *Mater Sci Eng* 2015;84:012100.
- [234] Chen D, Wang J, Zhang C. Coupled phase-field model and CFD for hot cracking predictions of Al-Li alloys. *Comput Mater Sci* 2021;192:110361.
- [235] Beckermann C. Modelling of macrosegregation: applications and needs. *Int Mater Rev* 2002;47(5):243–61.
- [236] Nadella R, Eskin DG, Du Q, Katgerman L. Macrosegregation in direct-chill casting of aluminium alloys. *Progr Mater Sci* 2008;53:421–80.
- [237] Garipey B, Caron Y. Investigations of the effect of casting parameters on the extent of centerline macrosegregation in DC cast sheet ingots. In *Light Metals*, Warrendale; 1991.
- [238] Eskin DG, Zuidema J, Savran VI, Katgerman L. Structure formation and macrosegregation under different process conditions during DC casting. *Mater Sci Eng* 2004;348A:232–44.
- [239] Bennon WD, Incropera FP. A Continuum Model for Momentum, Heat and Species Transport in Binary Solid-Liquid Phase Change Systems—I. Model Formulation. *Int J Heat Mass Transfer* 1987;30:2161–70.
- [240] Prescott PJ, Incropera FP. Modeling of dendritic solidification systems: reassessment of the continuum momentum equation. *Int J Heat Mass Transfer* 1991;34: 2351–9.
- [241] Voller VR, Brent AD. The modelling of heat, mass and solute transport in solidification systems. *Int J Heat Mass Transfer* 1989;3:1719–31.
- [242] Ni J, Incropera FP. Extension of the continuum model for transport phenomena occurring during metal alloy solidification—I. The conservation equations. *Int J Heat Mass Transfer* 1995;38:1271–84.
- [243] Krane MJM, Incropera FP. A scaling analysis of the unidirectional solidification of a binary alloy. *Int J Heat Mass Transfer* 1996;39:3567–79.
- [244] Krane MJM, Incropera FP. Solidification of ternary metal alloys—I. Model development. *Int J Heat Mass Transfer* 1997;40(16):3827–35.
- [245] Krane MJM, Incropera FP. Solidification of ternary metal alloys—II. Predictions of convective phenomena and solidification behavior in Pb-Sb-Sn alloys. *Int J Heat Mass Transfer* 1997;40(16):3837–47.
- [246] Thuinet L, Combeau H. Prediction of macrosegregation during the solidification involving a peritectic transformation for multicomponent steels. *J Mater Sci* 2004;39:7213–9.
- [247] Dore X, Combeau H, Rappaz M. Modelling microsegregation in ternary alloys: application to the solidification of Al-Mg-Si. *Acta Mater* 2000;48:3951–62.
- [248] Combeau H, Drezet J-M, Mo A, Rappaz M. Modelling of microsegregation in macrosegregation calculations. *Metall Mater Trans A* 1996;27A:2314–26.
- [249] Chen Q, Sundman B. Computation of partial equilibrium solidification with complete interstitial and negligible substitutional solute back diffusion. *Mater Trans* 2002;43(3):551–9.
- [250] Heyvaert L, Bedel M, Založnik M, Combeau H. Modeling of the Coupling of Microstructure and Macrosegregation in a Direct Chill Cast Al-Cu Billet. *Metall Mater Trans* 2017;48A:4713–34.
- [251] Založnik M, Xin S, Sarler B. Verification of a numerical model of macrosegregation in direct chill casting. *Int J Numer Methods Heat Fluid Flow* 2008;18: 308–24.
- [252] Venneker BCH, Katgerman L. Macrosegregation during DC casting of aluminium alloys: Numerical issues and the effect of metal entry. In *MCWASP IX*, Warrendale; 2000.
- [253] Venneker BCH, Katgerman L. Modelling issues in macrosegregation predictions in direct chill castings. *J of Light Metals* 2002;2:149–59.
- [254] Du Q, Eskin DG, Katgerman L. Numerical issues in modelling macrosegregation during DC casting of a multi-component aluminium alloy. *Int J Numer Methods Heat&Fluid Flow* 2009;19:917–30.
- [255] Hatic V, Mavric B, Sarler B. Simulation of macrosegregation in direct-chill casting- A model based on meshless diffuse approximate method. *Eng Anal Bounda Elem* 2020;113:191–203.
- [256] Hatic V, Mavric B, Sarler B. Simulation of a macrosegregation benchmark with a meshless diffuse approximate method, *Int. J Numer Methods Heat Fluid Flow* 2018;28(2):361–80.
- [257] Williams AJ, Croft TN, Cross M. Modeling of ingot development during the start-up phase of direct chill casting. *Metall Mater Trans* 2003;34B:727–34.
- [258] Fezi K, Plotkowski A, Krane MJM. Macrosegregation modeling during direct-chill casting of aluminum alloy 7050. *Numer Heat Transfer Part A* 2016;2016(9): 939–63.
- [259] Chen Q, Li H, Shen H. Transient Modeling of Grain Structure and Macrosegregation during Direct Chill Casting of Al-Cu Alloy. *Processes* 2019;7:333.
- [260] Combeau H, Bellet M, Fautrelle Y, Gobin D, Arquis E, Budenkova O, et al. A numerical benchmark on the prediction of macrosegregation in binary alloys. *Suppl Proc: Mater Fabr, Proper Charact Modell* 2011;2:755–62.
- [261] Vreeman CJ, Krane MJM, Incropera FP. The effect of free-floating dendrites and convection on macrosegregation in direct chill cast aluminum alloys: Part I: model development. *Int J Heat Mass Transfer* 2000;43:677–86.
- [262] Hatic V, Citernas Fernandez M, Mavric B, Založnik M, Combeau H. Simulation of a macrosegregation benchmark in a cylindrical coordinate system with a meshless method. *Int J Thermal Sciences* 2019;142:121–33.
- [263] Založnik M, Sarler B. Modeling of macrosegregation in direct-chill casting of aluminum alloys: Estimating the influence of casting parameters. *Mat Sci Eng A* 2005;413A:85–91.
- [264] Vreeman CJ, Schloz JD, Krane MJM. Direct Chill Casting of Aluminum Alloys: Modeling and Experiments on Industrial Scale Ingots. *J Heat Transfer* 2002;124: 947–53.

- [265] Du Q, Eskin DG, Katgerman L. Modeling macrosegregation during direct-chill casting of multicomponent aluminum alloys. *Metall Mater Trans A* 2007;38A:180–9.
- [266] Vreeman CJ, Krane MJM, Incropera FP. The effect of free-floating dendrites and convection on macrosegregation in direct chill cast aluminum alloys: Part II: predictions for Al–Cu and Al–Mg alloys. *Int J Heat Mass Transfer* 2000;43:687–704.
- [267] Zaloznik M, Sarler B. Thermosolutal flow in metals and implications for DC casting. In *MCWASP XI*, Warrendale; 2006.
- [268] Pakanati A, M'Hamdi M, Combeau H, Zaloznik M. Modelling macrosegregation modification in dc casting of aluminium alloys in sheet ingots accounting for inlet melt flow, equiaxed grain morphology and transport. *Mater Sci Eng* 2020;861:012040.
- [269] Pakanati A, Tveit K, M'Hamdi M, Combeau H, Zaloznik M. Analysis of the Interplay Between Thermo-solutal Convection and Equiaxed Grain Motion in Relation to Macrosegregation Formation in AA5182 Sheet Ingots. In *Light Metals 2020*, Warrendale; 2019.
- [270] Tveit K, Pakanati A, M'Hamdi M, Combeau H, Zaloznik M. A Simplified Three-Phase Model of Equiaxed Solidification for the Prediction of Microstructure and Macrosegregation in Castings. *Metall Mater Trans A* 2018;49:2778–94.
- [271] Pakanati A, Tveit K, M'Hamdi M, Combeau H, Zaloznik M. Application of an equiaxed grain growth and transport model to study macrosegregation in a DC casting experiment. *Metall Mater Trans A* 2019;50A:1773–86.
- [272] Zhang L, Eskin DG, Miroux A, Subroto T, Katgerman L. Effect of inlet geometry on macrosegregation during the direct chill casting of 7050 alloy billets: experiments and computer modelling. *IOP Conference Series* 2012;33:012019.
- [273] Hess JB. Physical metallurgy of recycling wrought aluminum alloys. *Metall Trans A* 1983;14:323–7.
- [274] Taylor AT, Thompson DH, Wegner JJ. Direct Chill Casting of Large Aluminium Ingots. *Met Prog* 1957;72(5):70–4.
- [275] Dassel JL, Zinniger TC. Sheet ingot casting with inflatable wipers, in *Light Metals*. USA: Dallas TX; 1982.
- [276] Lalpoor M, Eskin DG, Katgerman L. Fracture behaviour and mechanical properties of high strength aluminium alloys in the as-cast condition. *Mater Sci Eng A* 2008;497:186–94.
- [277] Boender W, Burghardt A. Application of fracture mechanics to the DC casting of high-strength aluminium alloys. In *Solidification Processing*, Sheffield; 2007.
- [278] Ludwig O, Drezet JM, Commet B, Heinrich B. Modelling of internal stresses in DC casting and sawing of high strength aluminium slabs. In *MCWASP XI*, Warrendale; 2006.
- [279] Lalpoor. Study of cold cracking during DC casting of high-strength aluminium alloys. Delft: PhD Thesis TUDelft; 2010.
- [280] Zabarar N, Voller VR. Numerical strategies for thermomechanical analysis of castings. In *MCWASP IV*, Warrendale; 1988.
- [281] Kumar A, Nallathambi M, Tyagi E Specht, Bertram A. Thermomechanical analysis of direct chill casting using finite element method. *Trans Indian Inst Metals* 2011;64:13–9.
- [282] Li HX, Bai QL, Li Y, Du Q, Katgerman L, Zhang JS, et al. Mechanical properties and cold cracking evaluations of four 7xxxseries aluminum alloys using a newly developed index. *Mater Sci Eng A* 2017;698:230–7.
- [283] Lalpoor M, Eskin DG, Katgerman L. Cold cracking assessment in AA7050 billets during direct-chill casting by thermomechanical simulation of residual thermal stresses and application of fracture mechanics. *Metall Mater Trans A* 2009;40:3304–13.
- [284] Tada H, Paris PC, Irwin GR. The stress analysis of cracks handbook. 3rd ed., New York: ASME Press; 2000.
- [285] Drezet J-M, Phillion A. As-cast residual stresses in an aluminum alloy AA6063 billet: Neutron diffraction measurements and finite element modeling. *Met Mater Trans A* 2010;41:3396–404.
- [286] Drezet J-M, Pirling T. Influence of a wiper on residual stresses in AA7050 rolling plate ingots. *J Mater Proc Techn* 2014;214:1372–8.
- [287] Lalpoor M, Eskin DG, Katgerman L. Cold cracking development in AA7050 direct chill-cast billets under various casting conditions. *Metall Mater Trans A* 2010;41:2425–34.
- [288] Lalpoor M, Eskin DG, Ruvalcaba D, Fjaer HG, Ten Cate AON, Katgerman L. Cold cracking in DC-cast high strength aluminum alloy ingots: An intrinsic problem intensified by casting parameters. *Mater Sci Eng A* 2011;528:2831–42.
- [289] Sosro Subroto TA. Connection between hot tearing and cold cracking in DC-casting of AA7050. Delft: PhD Thesis, TU Delft; 2014.
- [290] Bounds SM, Moran GJ, Pericleous KA, Cross M. Finite volume modelling of shrinkage porosity formation in metal. In *Modelling of Casting Welding and Advanced Solidification Processes VIII*, Warrendale, PA, USA; 1998.
- [291] Esser P, Schankies C, Khalajzadeh V, Beckermann C. Advanced modeling of shrinkage porosity in castings. *Modelling of Casting, Welding and Advanced Solidification Processes XV*, Bristol, UK. 2020.
- [292] Sultana N, Rafiquzzaman M, Rahman Y, Das A. Solidification and Filling Related Defects Analysis Using Casting Simulation Technique with Experimental Validation. *Int J Mech Eng Appl* 2018;6(6):150–60.
- [293] Campbell J. Casting non-ferrous metals. UK Patent 2122523; 1983.
- [294] Fox S, Campbell J. Visualisation of Oxide Film Defects During Solidification of Aluminium Alloys. *Scr Mater* 2000;43:881–6.
- [295] Campbell J. Invisible macrodefects in castings. *Journal de Physique IV, Colloque C7*, supp. to *J Phys III* 1993;3:861–71.
- [296] Chen Y-J, Teng H-Y, Tsai Y-T. Diagnosis of oxide films in cast aluminum alloys. *J Mater Eng Perform* 2004;13:69–77.
- [297] El-Sayed MA. The Behaviour of Bifilm Defects in Cast Al-7Si-Mg Alloy. *PLoS ONE* 2016;11(8).
- [298] Reilly C, Green NR, Jolly MR. Surface oxide film entrainment mechanisms in shape casting running systems. *Metall Mater Trans B* 2009;40(6):850–8.
- [299] Chen Q. The Effect of Transition Metal Additions on Double Oxide Film Defects in Al Alloy., Birmingham; 2016.
- [300] Gyamarti G, Fegyverneki GY, Tokar M, Mende T. Investigation on Double Oxide Film Initiated Pore Formation in Aluminum Casting Alloys. *Int J Eng Manage Sci* 2020;141–53.
- [301] Runyoro JJ, Boutorabi SMA, Campbell J. Critical gate velocities for film forming alloys: a basis for process specification. *Trans Am Found Society* 1992;100:225–34.
- [302] Yang X, Huang X, Dai X, Campbell J, Tatler J. Numerical modelling of entrainment of oxide film defects in filling of aluminium alloy castings. *Int J Cast Met Res* 2004;17(6):321–31.
- [303] Reilly C, Green NR, Jolly MR. Surface oxide film entrainment mechanisms in shape casting running systems. *Metall Mater Trans B* 2009;40.
- [304] Jolly MR, Reilly C, Green N. Investigating surface entrainment events using CFD for the assessment of casting filling methods. *Modelling of Casting, Welding and Advanced Solidification Processes XII*, Warrendale, PA, USA. 2009.
- [305] Reilly C, Green NR, Jolly MR. The modelling of oxide film entrainment in casting systems using computational modelling. *Appl Math Model* 2013;37(18–19):8451–66.
- [306] Duan J. Physical and computational models of free surface related defects in low-pressure die-cast aluminum alloy wheels. Canada: Vancouver; 2011.
- [307] Reilly C, Green NR, Jolly MR. The present state of modeling entrainment defects in the shape casting process. *Appl Math Model* 2013;37(3):611–28.
- [308] Prakash M, Cleary P, Granfield J. Modelling of metal flow and oxidation during furnace emptying using smoothed particle hydrodynamics. *J Mater Process* 2009;209(7):3396–407.
- [309] Reilly C, Green NR, Jolly MR. State of the Art Review of Modelling Entrainment Defects in the Shape Casting Process. 4th International Conference on Shape Casting. Wiley; 2011.
- [310] Lai NW, D GW, Campbell J. Modelling of the potential for oxide film entrainment in light metal alloy castings. In *Modelling of casting, welding and advanced solidification process X*, Warrendale, PA, USA; 2003.
- [311] Barkhudarov MR, Hirt CW. Tracking Defects. In *1st International Aluminium Casting Technology Symposium*, Rosemont; 1998.
- [312] Massey BS. *Mechanics of Fluids*. 6th ed. London: Chapman and Hall; 1992.
- [313] Cuesta R, Delgado A, Maroto A, Mozo D. Numerically modelling oxide entrainment in the filling of castings: the effect of the Webber Number. *J Mater* 2006;58:62–5.
- [314] Isawa T. The control of the initial fall of liquid metal in gravity filled casting systems, Birmingham; 1993.
- [315] Hsu F-Y. Further Developments of Running Systems for Aluminium Castings, Birmingham; 2003.

- [316] Griffiths WD, Beshay Y, Caden AJ, Fan X, Gargiuli J, Leadbeater TW, et al. The use of positron emission particle tracking (PEPT) to study the movement of inclusions in low-melting-point alloy castings. *Mater Trans B* 2012;43.
- [317] Tomiyama A, Zun I, Higaki H, Makino Y, Sakaguchi T. A Three - Dimensional Particle Tracking Method for Bubbly Flow Simulation. *Nucl Eng Des* 1997;175: 77–86.
- [318] Jakumeit J, Goodheart K, Albers M. Influence of gas phase on mould filling for sand casting. In *Modelling of casting, welding and advanced solidification process XII*, Vancouver; 2009.
- [319] Kimatsuka A, Kuroki Y. Mold Filling Simulation for Predicting Gas Porosity. *IHI Engineering Review* 2007;40(2):83–8.
- [320] Majidi SH, Beckermann C. Modelling of air entrainment during pouring of metal castings. *Int J Cast Metals Res* 2017;30(5):301–15.
- [321] Flow Science. Flow 3D: Air Entrainment; 2020. [Online]. Available: <https://www.flow3d.com/modeling-capabilities/air-entrainment/> [Accessed 6 August 2020].
- [322] Pavlak L, Sturm JC. Magma GmbH, Reduction of Oxide Inclusions in Aluminum Cylinder Heads through Virtual Design of Experiments; 2015. [Online]. Available: [https://www.magma-soft.com/export/shared/galleries/pdfs\\_publications/2015\\_MAGMA\\_ReductionOxideInclusionsAluminumCylinderHeadsDOE.pdf](https://www.magma-soft.com/export/shared/galleries/pdfs_publications/2015_MAGMA_ReductionOxideInclusionsAluminumCylinderHeadsDOE.pdf) [Accessed 6 August 2020].
- [323] Papanikolaou M, Pagone E, Jolly MR, Salonitis K. Numerical Simulation and Evaluation of Campbell Running and Gating Systems. *Metals* 2020;10, no. 1:68.